Synergistic Role of Protein Phosphatase Inhibitor 1 and Sarco/Endoplasmic Reticulum Ca^{2+}-ATPase in the Acquisition of the Contractile Phenotype of Arterial Smooth Muscle Cells

Larissa Lipskaia, PhD; Regis Bobe, PhD; Jiqiu Chen, MD; Irene C. Turnbull, MD; Jose J. Lopez, PhD; Elise Merlet, PhD; Dongtaq Jeong, PhD; Ioannis Karakikes, PhD; Alexandra S. Ross, BS; Lifan Liang, MD; Nathalie Mougenot, PhD; Fabrice Atassi, MsC; Anne-Marie Lompré, PhD; Sima T. Tarzami, PhD; Jason C. Kovacic, MD; Evangelia Kranias, PhD; Roger J. Hajjar, MD; Lahouaria Hadri, PhD

Background—Phenotypic modulation or switching of vascular smooth muscle cells from a contractile/quiescent to a proliferative/synthetic phenotype plays a key role in vascular proliferative disorders such as atherosclerosis and restenosis. Although several calcium handling proteins that control differentiation of smooth muscle cells have been identified, the role of protein phosphatase inhibitor 1 (I-1) in the acquisition or maintenance of the contractile phenotype modulation remains unknown.

Methods and Results—In human coronary arteries, I-1 and sarco/endoplasmic reticulum Ca^{2+}-ATPase expression is specific to contractile vascular smooth muscle cells. In synthetic cultured human coronary artery smooth muscle cells, protein phosphatase inhibitor 1 (I-1 target) is highly expressed, leading to a decrease in phospholamban phosphorylation, sarco/endoplasmic reticulum Ca^{2+}-ATPase, and cAMP-responsive element binding activity. I-1 knockout mice lack phospholamban phosphorylation and exhibit vascular smooth muscle cell arrest in the synthetic state with excessive neointimal proliferation after carotid injury, as well as significant modifications of contractile properties and relaxant response to acetylcholine of femoral artery in vivo. Constitutively active I-1 gene transfer decreased neointimal formation in an angioplasty rat model by preventing vascular smooth muscle cell contractile to synthetic phenotype change.

Conclusions—I-1 and sarco/endoplasmic reticulum Ca^{2+}-ATPase synergistically induce the vascular smooth muscle cell contractile phenotype. Gene transfer of constitutively active I-1 is a promising therapeutic strategy for preventing vascular proliferative disorders. **(*Circulation*. 2014;129:773-785.)**

Key Words: calcium ■ gene therapy ■ muscle, smooth ■ restenosis ■ vascular diseases

Vascular proliferative disorders such as primary atherosclerosis, restenosis after balloon angioplasty, vein-graft disease, and coronary arteriosclerosis are the most common causes of severe cardiovascular diseases, the current leading cause of death in the United States and the predicted number 1 killer worldwide by 2020.[1] Although vascular smooth muscle cells (VSMCs) are normally located in the arterial media and maintained in a contractile nonproliferative state in vivo, injury or mechanical stress of arteries causes migration of VSMCs into the intima layer of the arterial wall, where the VSMCs switch their phenotype and start to proliferate and synthesize extracellular matrix proteins, resulting in expansion of the arterial intima.[2–5]

Clinical Perspective on p 785

VSMC phenotype switch from a contractile/quiescent to a proliferative/synthetic one is associated with alterations of many components of the VSMC Ca^{2+} signaling network.[6] These changes in VSMC phenotype have been well characterized at the level of contractile proteins[7] and more recently at the level of Ca^{2+} handling proteins.[8] Indeed, expression levels of the L-type Ca^{2+} channel, sarco/endoplasmic reticulum

Received March 12, 2013; accepted November 8, 2013.

From the Cardiovascular Research Center. Mount Sinai School of Medicine, New York, NY (L. Lipskaia, J.C., I.C.T., D.J., I.K., A.S.R., L. Liang, S.T.T., J.C.K., R.J.H.., L.H.); INSERM UMRS 956, Université Pierre et Marie Curie-Paris 6, Paris, France (L. Lipskaia, E.M., F.A., A.-M.L.); LIA/Transatlantic Cardiovascular Research Center, Université Pierre et Marie Curie/Mount Sinai School of Medicine, New York, NY (L. Lipskaia, J.C., I.C.T., E.M., D.J., I.K., L. Liang, F.A., A.-M.L., S.T.T., J.C.K., R.J.H., L.H.); INSERM U770, University Paris Sud, Le Kremlin-Bicêtre, France (R.B., J.J.L.); PECMV-Université Pierre et Marie Curie-Paris, Paris, France (N.M.); and University of Cincinnati, Cincinnati, OH (E.K.).

The online-only Data Supplement is available with this article at http://circ.ahajournals.org/lookup/suppl/doi:10.1161/CIRCULATIONAHA.113.002565/-/DC1.

Correspondence to Lahouaria Hadri, PhD, Mount Sinai School of Medicine, Cardiovascular Research Center, Box 1030, 1470 Madison Ave, New York, NY 10029. E-mail lahouaria.hadri@mssm.edu

Circulation **is available at http://circ.ahajournals.org** **DOI: 10.1161/CIRCULATIONAHA.113.002565**

(SR) Ca^{2+}-ATPase (SERCA2a), and ryanodine receptor are decreased in synthetic VSMCs.[8–12] Importantly, a sustained increase in cytosolic Ca^{2+} is necessary to activate calcineurin, a Ca^{2+}/calmodulin-dependent serine/threonine-specific protein phosphatase 2B, which dephosphorylates many proteins, including nuclear factor of activated T cell (NFAT), that may translocate to the nucleus[13] and induce VSMC proliferation.[14]

Recently, we demonstrated that Ca^{2+} cycling in contractile VSMCs requires the expression of the SERCA2a isoform, whereas the Ca^{2+} cycling in synthetic VSMCs is associated only with the expression of the ubiquitous isoform SERCA2b.[15] Phospholamban (PLB), a negative regulator of SERCA2 activity, is inhibited by protein kinase A (PKA) phosphorylation and activated by protein phosphatase 1 (PP1)–dependent dephosphorylation.[16] However, inhibitor 1 (I-1), a ubiquitously expressed 28-kDa protein, is a highly specific inhibitor of PP1 that enhances both PKA-dependent PLB phosphorylation and therefore SERCA2 activity.[17–21] I-1 is a major player in multiple neurohormonal pathways associated with Ca^{2+} homeostasis and contractile function. On stimulation, PKA phosphorylates Thr35 in I-1, resulting in PP1 inhibition and amplification of the contractile response.[17,21,22] Inactivation of I-1 occurs by dephosphorylation of Thr35 by protein phosphatase 2A and 2B, leading to the reversal of PP1 inhibition and restoration of basal function.[23,24] I-1 can also be phosphorylated at Ser67 and Thr75 by phosphokinase C, but these phosphorylations enhance PP1 activity and diminish contractility.[25–27] In VSMCs, regulation of phosphoprotein phosphatases has been shown to be a major component in the Ca^{2+} sensitization of contraction.[28] Of relevance, I-1 is present in VSMCs[29]; however, studies of its role in modulating VSMC function have provided conflicting results.[20,30] In light of the high expression of I-1 in these cells, other functions for I-1 in VSMCs are a strong possibility.

The goal of this study was to elucidate the role of PKA signaling enhancer I-1 in the control of VSMC Ca^{2+} cycling and phenotypic modulation. Here, we demonstrate that I-1 and SERCA2a act synergistically on Ca^{2+} cycling and contribute directly to the VSMC contractile phenotype. Gene transfer of constitutively active I-1 (I-1c) may be a promising therapeutic strategy for preventing vascular proliferative disorders.

Methods

Please refer to the expanded Methods section in the online-only Data Supplement for a detailed description.

Human Samples

Fragments of the left anterior descending coronary artery were dissected from human explanted hearts, and unused segments of left internal mammary artery from 5 patients were obtained during coronary artery bypass from the Surgical Department of the Cardiology Institute at Pitié-Salpêtrière Hospital, Paris, France, in accordance with French bioethical laws (L.1211-3-9). The artery segments were immediately immersed in physiological saline solution, placed at 4°C, and processed within 2 to 3 hours.

Animals

Genetically modified I-$1^{-/-}$ mice[31] were used. C57 Bl-6 mice (Charles River) of the same age were used as nonlittermate controls. Adult male Sprague-Dawley rats (Charles River) were used for the in vivo carotid injury model and for isolation of aortic VSMCs. Animals were treated according to institutional guidelines.

Measurement of I-I Knockout Femoral Artery Contraction and Relaxation

Mice were anesthetized with a mixture of ketamine (65 mg/kg) and xylazine (13 mg/kg, IP). The left femoral artery was dissected gently, and a 7-0 nylon suture (Ethicon, Johnson & Johnson) was placed under the vessel to serve as reference to calculate vessel diameter. The vessel was equilibrated by adding 100 μL PBS to the perivascular site for 5 minutes. Prostaglandin F2α (1 mmol/L, 100 μL, Sigma P0314) was applied locally on the vessel to contract the artery. After 10 minutes, the prostaglandin F2α solution was removed, and 100 μL acetylcholine (10^{-9} to 10^{-3} mol/L, Sigma A6625-25G) was added cumulatively to the vessel with 5-minute interval. The change of vessel diameter was recorded with a pixel link camera, and measurements were performed using Image-J.

Measurement of $[Ca]^{2+}_i$

Cells were loaded with 2 μmol/L Fura-2-AM for 45 minutes at 37°C and kept in serum-free medium for 30 minutes before experimentation. HEPES buffer (in mmol/L: 116 NaCl, 5.6 KCl, 1.2 $MgCl_2$, 5 $NaHCO_3$, 1 NaH_2PO_4, 20 HEPES, pH 7.4) was used for the experiments. To increase the rate up 7 images per second, single images of fluorescent emission at 510 nm under single excitation at 380 nm were recorded. Changes in $[Ca^{2+}]_i$ in response to the indicated agonist were calculated either using the ratio 380em/380em (basal) or the ratio (340em/380em)/(340em[basal]/380em [basal]). For each recorded images, 3 distinct regions of interest with no cells were selected, the means of fluorescence measured for these 3 areas were used as a background, and subtraction was applied for each cell measurement before any further calculation.

Statistical Analysis

All quantitative data are presented as the mean±SEM of at least 3 independent experiments. Data were analyzed by use of the Kruskal-Wallis test with a Dunn adjustment for multiple comparisons. Statistical comparisons of 2 groups were analyzed by Wilcoxon matched-pairs signed-rank test or the Mann-Whitney nonparametric test. Linear mixed-effect models with random intercepts were used to analyze the femoral artery contraction and relaxation percent change. Differences were considered significant when $P<0.05$. Data were analyzed with GraphPad Prism 5 software and IBM SPSS Statistics software.

Results

Regulation of the I-1/PP1/PLB/SERCA Signaling Axis in Contractile Versus Synthetic Human VSMCs

Because VSMCs have the capacity for phenotypic dedifferentiation from a contractile to synthetic phenotype, we assessed whether the I-1/PP1 signaling pathway was modified during this process. First, we analyzed I-1 expression in contractile and synthetic VSMCs from healthy segments of human coronary arteries (hCAs) obtained from 5 patients with dilated (nonischemic) cardiomyopathy. hCAs contain a subendothelial layer of synthetic VSMCs and connective tissue to support the endothelium, whereas the medial layer is composed mainly of contractile VSMCs.[15] I-1 protein was expressed only in the medial layers of hCAs (Figure 1A and Figure IA in the online-only Data Supplement) and mammary arteries (Figure IB in the online-only Data Supplement) and was downregulated in the subendothelial layer (Figure 1A) and in the media of atherosclerotic vessels (Figure IC in the online-only Data Supplement), suggesting that I-1 is specifically highly expressed in contractile VSMCs.[15] Immunoblot analysis

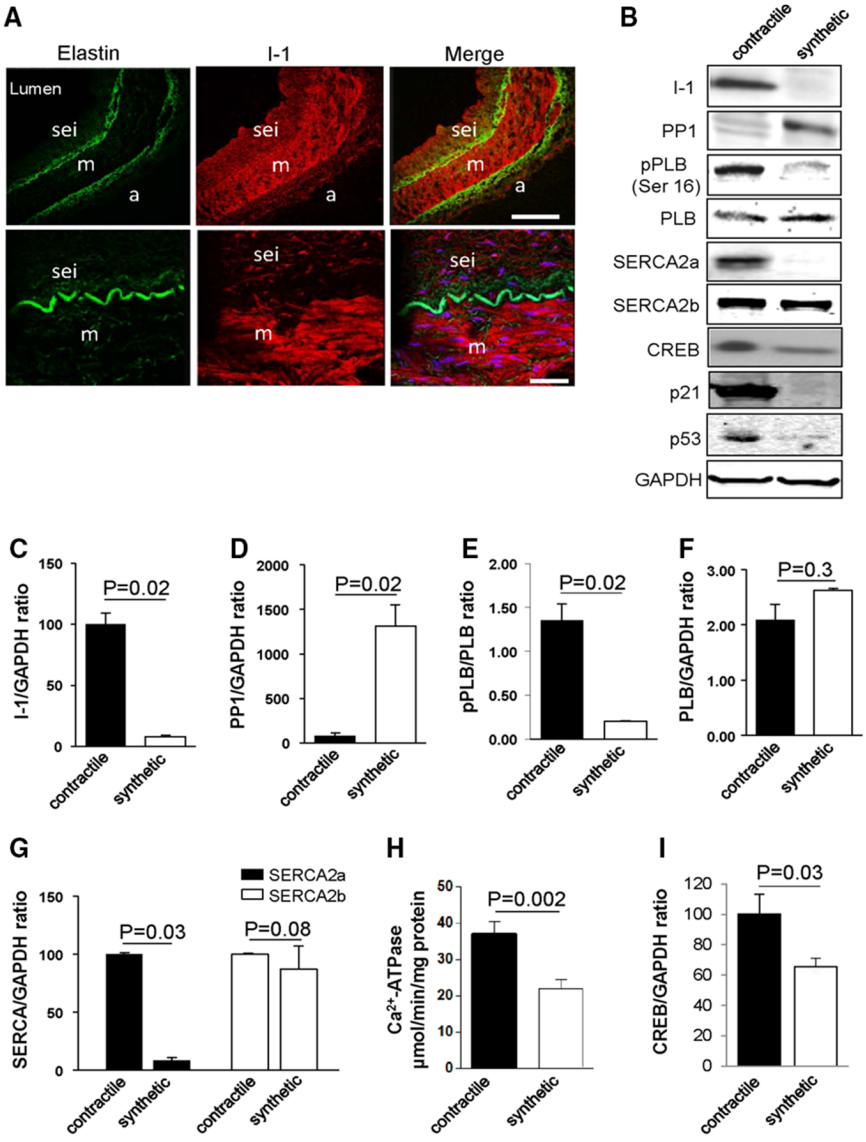

Figure 1. Modulation of inhibitor 1 (I-1)/protein phosphatase 1 (PP1)/phospholamban (PLB)/sarco/endoplasmic reticulum calcium-ATPase (SERCA) signaling pathway within contractile and synthetic human coronary artery smooth muscle cells (hCASMCs). **A**, Confocal immunofluorescence microscopy of healthy human coronary artery (hCA) cross sections showing I-1 (red) and elastin autofluorescence (green). a Indicates adventitia; m, media; and sei, subendothelial neointima. Scale bar, 20 and 50 μm. **B**, Immunoblot analysis of indicated proteins in contractile hCAs and synthetic (cultured) hCASMCs. CREB indicates cAMP-responsive element binding; and pPLB, PLB phosphorylated on Ser16. **C** through **I**, Histograms showing the relative ratio of I-1, PP1, SERCA2a and SERCA2b, and CREB expression normalized to GAPDH in 3 independent experiments. **E**, Relative pPLB level was determined through normalization to total PLB level. **H**, SERCA activity measured in contractile and synthetic (cultured) vascular smooth muscle cells (VSMCs).

performed on VSMCs of the medial layer of hCAs (contractile cells) and cultured human coronary artery smooth muscle cells (hCASMCs; synthetic cells) confirmed a higher expression of I-1 in the contractile cells compared with hCASMCs (Figure 1B and 1C), whereas its target, total PP1, was upregulated and highly detectable by immunofluorescence in synthetic hCASMCs (Figure 1B and 1D and Figure IIA in the online-only Data Supplement). Next, we looked to PP1 isoform expression in synthetic versus contractile VSMCs by coimmunostaining with smooth muscle α-actin. PP1α was detected only in the nucleus; however, PP1β was abundantly expressed in synthetic VSMCs with a higher level in the nucleus and in the cytosol compared with the contractile VSMCs (Figure IIB and IIC in the online-only Data Supplement, respectively). Consequently, PLB phosphorylation was higher in contractile VSMCs compared with synthetic VSMCs (Figure 1B and 1E), without a change in total PLB expression (Figure 1B and 1F). Confirming previous observations, SERCA2a was expressed only in contractile VSMCs,[15] whereas SERCA2b expression was similar between contractile and synthetic VSMCs (Figure 1B and 1G). In agreement with this pattern of activity in the I-1/PP1/PLB/SERCA signaling pathway, global SR Ca^{2+}-ATPase activity was significantly decreased in synthetic VSMCs compared with contractile VSMCs (Figure 1H). The decrease in SR Ca^{2+}-ATPase activity in synthetic VSMCs can be linked to the lack of SERCA2a expression and to the inhibitory effect of unphosphorylated PLB on SR Ca^{2+}-ATPase. In addition, the expression of other markers of quiescent status such as cAMP-responsive element binding (CREB; Figure 1B and 1I), p53 (tumor suppressor gene), and p21 was also markedly reduced in synthetic SMCs (Figure 1B).

Loss of I-1 Leads to a Shift From Contractile to Synthetic VSMC Phenotype

To study the impact of the loss of I-1 on the VSMC phenotype, thoracic aortas of adult (6-month-old) I-1$^{-/-}$ mice (I-1 knockout [KO]) and control mice (wild type [WT]) were analyzed by immunoblot with specific markers. Immunoblot analysis and immunostaining in aortic cross sections confirmed the loss of I-1 expression in the thoracic aortas from I-1 KO

compared with WT mice (Figure 2A–2C). Interestingly, PP1 expression was markedly increased in I-1 KO compared with WT mice (Figure 2A and 2D), which was consistent with reduced PLB phosphorylation (Figure 2A and 2E). SERCA2a protein expression was also significantly decreased in I-I KO aortic VSMCs (Figure 2A and 2F), whereas SERCA2b level remained unchanged (Figure 2A and 2G). A marked decrease in SR Ca^{2+}-ATPase activity in I-1 KO mice thoracic aorta compared with WT mice was observed (Figure 2H), recapitulating the observations in human samples (Figure 1).

Next, we analyzed the expression of markers of differentiated SMCs. We found that by immunoblot and immunostaining

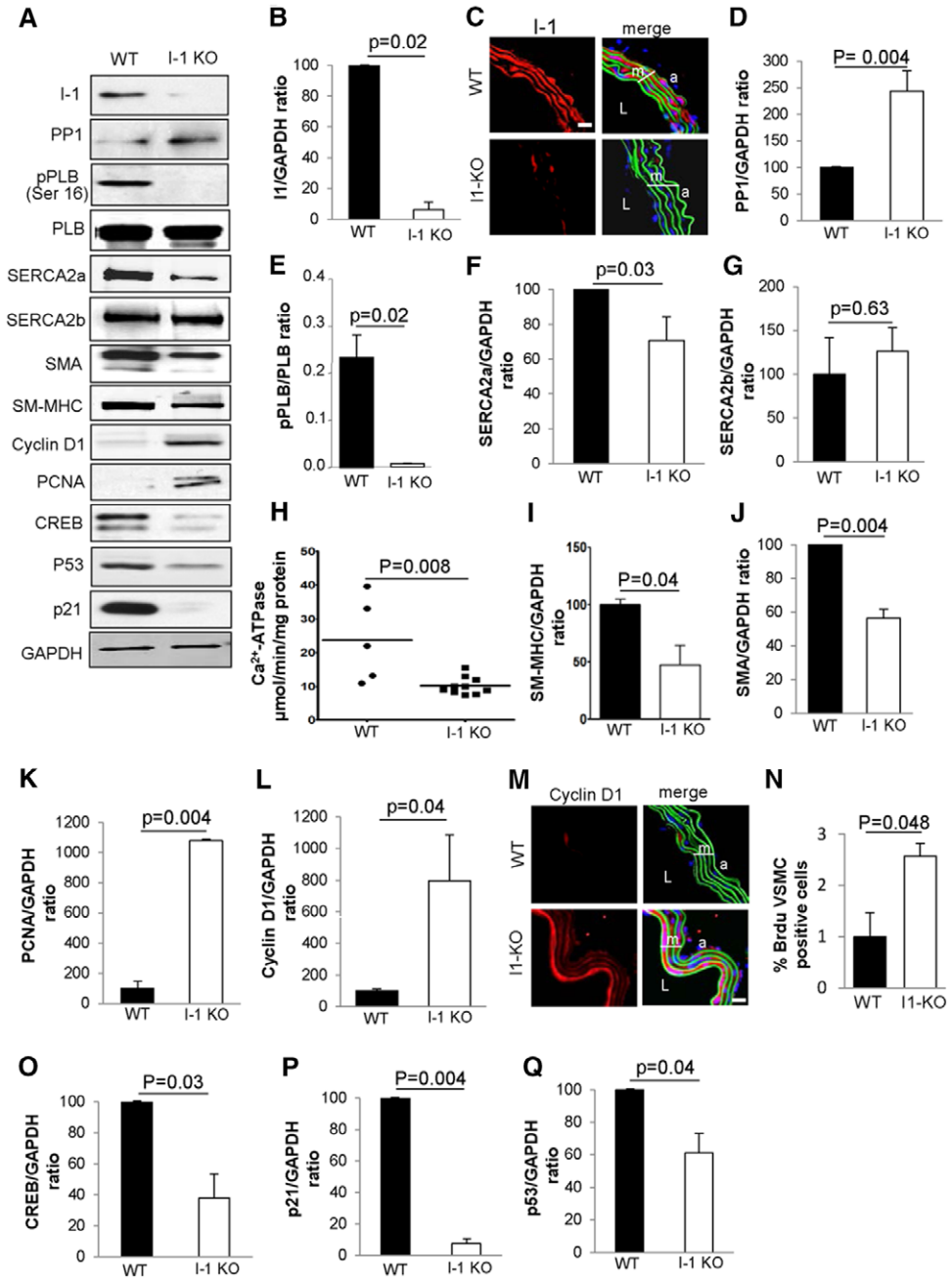

Figure 2. Phenotype analysis and sarco/endoplasmic reticulum (SR) Ca^{2+}-ATPase activity of vascular smooth muscle cells (VSMCs) from thoracic aortas of wild-type (WT) and inhibitor 1 knockout (I-1 KO) mice. **A**, Immunoblot analysis of the indicated proteins in the media of thoracic aortas from adult (6-month-old) WT and I-1 KO mice. Three aortas were used for preparation of each sample. **B, D, F** through **L,** and **O** through **Q**, Histograms showing the relative ratio of I-1, protein phosphatase 1 (PP1), sarco/endoplasmic reticulum calcium-ATPase (SERCA) 2a, SERCA2b, smooth muscle α-actin (SMA), smooth muscle myosin heavy chain (SM-MHC), proliferating cell nuclear antigen (PCNA), cyclin D1, cAMP-responsive element binding (CREB), p53, and p21 expression normalized to GAPDH in 3 independent experiments. **E**, Relative phospholamban phosphorylation (pPLB) levels were determined by normalization to total PLB. Data represent mean±SEM of 3 independent experiments. **H**, SR Ca^{2+}-ATPase activity measured on thoracic aortas from WT (n=5) and I-1 KO (n=10) mice. **C** and **M**, Immunostaining of I-1 and cyclin D1 in the media of thoracic aortas from WT and I-1 KO mice, respectively. Scale bar, 20 μm. a Indicates adventitia; L, lumen; and m, media. **N**, Quantification of proliferating aorta BrdU-positive VSMCs from adult 6-month-old WT (n=3) and I-1 KO (n=4) mice. Data represent mean±SEM.

analysis, smooth muscle myosin heavy chain (SM-MHC) and smooth muscle α-actin, markers of contractile VSMCs, were highly expressed in WT aortic VSMCs but were significantly decreased in I-1 KO aortic VSMCs (Figure 2A, 2I, and 2J, respectively, and Figure IIIA and IIIC in the online-only Data Supplement, respectively). In I-1 KO aortic VSMCs, the few I-1–positive cells (green) were SM-MHC–positive cells (red; Figure IIIB in the online-only Data Supplement). Calponin was also decreased in the medial I-1 KO aortic VSMCs (Figure IIID in the online-only Data Supplement). Markers of proliferating cells such as proliferating cell nuclear antigen were absent in the aortic VSMCs of WT mice, in agreement with their quiescent status compared with I-1 KO mice (Figure 2A and 2K). In addition, cyclin D1 was significantly increased in I-1 KO mice aortic VSMCs (Figure 2A and 2L). Immunolabeling performed on thoracic aortic cross sections confirmed the presence of abundant cyclin D1–expressing proliferating cells on the luminal vessel border (Figure 2M), with an increase in NFATC3 expression compared with WT (Figure IIIE in the online-only Data Supplement) and a significantly higher proportion of BrdU-positive VSMCs in I-1 KO compared with WT mice (Figure 2N). Furthermore, expression levels of CREB, p53, and p21 were significantly decreased in the aortic VSMCs of I-1 KO mice (Figure 2A, 2O, 2P, and 2Q, respectively). These data likely indicate that the downregulation of these key modulators of SMC contraction in the aorta of I-1 KO mice reflects the shift between contractile and synthetic phenotypes and suggests that the loss of I-1 affects the differentiation of VSMCs and their ability to adjust the phenotype to the physiologically required contractile state. Apoptosis was also evaluated in aortic cross sections from I-1 KO and WT aortas using terminal deoxynucleotidyl transferase dUTP nick-end labeling. Numerous apoptotic cells were detected in the media of I-1 KO aortas compared with WT aortas (Figure IIIF in the online-only Data Supplement).

Moreover, morphometric analysis revealed a marked increase in thoracic aortic thickness in I-1 KO mice (Figure 3A and 3B). The phenotype observed in the vascular cells of I-1 KO mice, characterized by anarchic proliferation and apoptosis, can be described as a vascular proliferative disorder. We further investigated the proliferative capacities of VSMCs lacking I-1. To achieve this, left carotid artery injury with and without I-1c gene transfer was performed in adult (12 weeks old) WT and I-1 KO mice. The right carotid artery from WT was used as sham operated (no wire injury). One month after surgery, histological analysis revealed the presence of neointimal lesions in injured arteries of both mouse strains. Of note, the medial thickness of the carotid artery was already increased in noninjured carotids from I-1 KO mice (Figure 3C and 3D), confirming the observations made from thoracic aortas (Figure 3B). As expected, carotid injury induced medial and neointimal proliferation in both strains (Figure 3D and 3E), but the thickness was significantly greater in I-1 KO animals (Figure 3E). Overexpression of a truncated, constitutively active form of I-1 by an adenovirus (Ad.I-1c) by gene transfer markedly reduced the neointimal thickness in the injured WT carotid artery compared with WT nontransduced animals (Figure 3D and 3E). However, I-1c–infected I-1 KO did not significantly reduce postinjury neointimal proliferation, nor did it reduce medial cell proliferation compared WT I1c-infected mice (Figure 3D and 3E), probably as a consequence of VSMC dedifferentiation. Analysis by immunofluorescence confirmed that injured left carotid arteries transduced with I-1c showed downregulation of markers of the contractile VSMCs phenotype such as SM-MHC and SERCA2a in I-1 KO mice compared with sham noninjured and WT infected carotid arteries after injury (Figure IV in the online-only Data Supplement). These data demonstrate that VSMCs lacking I-1 proliferate readily and appear unable to adopt a quiescent state. Consistent with this, adult I-1–deficient mice develop a vascular proliferative disorder with excessive neointimal proliferation after vascular injury.

To assess the effects of I-1 gene ablation on endothelium-dependent contraction, mouse femoral arteries were stimulated with 1 μmol/L prostaglandin F2α, and measurements of outer vessel diameter were performed at different time points and compared with baseline (Figure 3F). Prostaglandin F2α, which is known to induce endothelium-dependent contractions,[32] resulted in significant modifications of contractile properties of femoral arteries of I-1 KO mice compared with WT (Figure 3F). Furthermore, analysis of the dose-response relationships to acetylcholine indicated a decrease in the strength of the response of the I-1 KO femoral arteries to endothelium-dependent relaxation at higher concentrations compared with WT mice (Figure 3G).

The Effect of I-1 on Calcium Signaling in VSMCs Is SERCA2 Isoform Dependent

To determine whether I-1–dependent PLB phosphorylation plays a role in the control of SR Ca^{2+} uptake and intracellular Ca^{2+} transient, we overexpressed Ad.I-1c in synthetic cultured hCASMCs.[21] Of note, the ubiquitous SERCA2b is the only isoform expressed in these cells (Figure 1B). The expression of I-1c protein was observed (7 kDa; Figure 4A, left), whereas endogenous I-1 (28 kDa) was not detectable in synthetic hCASMCs overexpressing I-1c (not shown). Adenovirus-mediated gene transfer of I-1c (Ad.I-1c) significantly increased PLB phosphorylation at Ser16 (Figure 4A). However, I-1c overexpression had no effect on hCASMC proliferation (Figure 4B), cyclin D1 expression (Figure VB in the online-only Data Supplement), and cell survival (Figure VC and VD in the online-only Data Supplement). Remarkably, when the cells were coinfected with Ad.I-1c and an adenovirus encoding for SERCA2a, PLB phosphorylation was significantly increased (Figure VA in the online-only Data Supplement), with a marked decrease in hCASMC proliferation (Figure 4B). These data indicate that to inhibit proliferation, I-1 needs the presence of SERCA2a.

Regulation of gene expression by Ca^{2+} can be mediated by Ca^{2+}-dependent phosphorylation of the transcription factor CREB.[33] Therefore, we hypothesized that I-1/CREB signaling might regulate the VSMC phenotype. In testing this hypothesis, we found that the expression levels of CREB phosphorylated on Ser133 and p21 were highly elevated in synthetic VSMCs co-overexpressing I-1c and SERCA2a (Figure VA in the online-only Data Supplement).

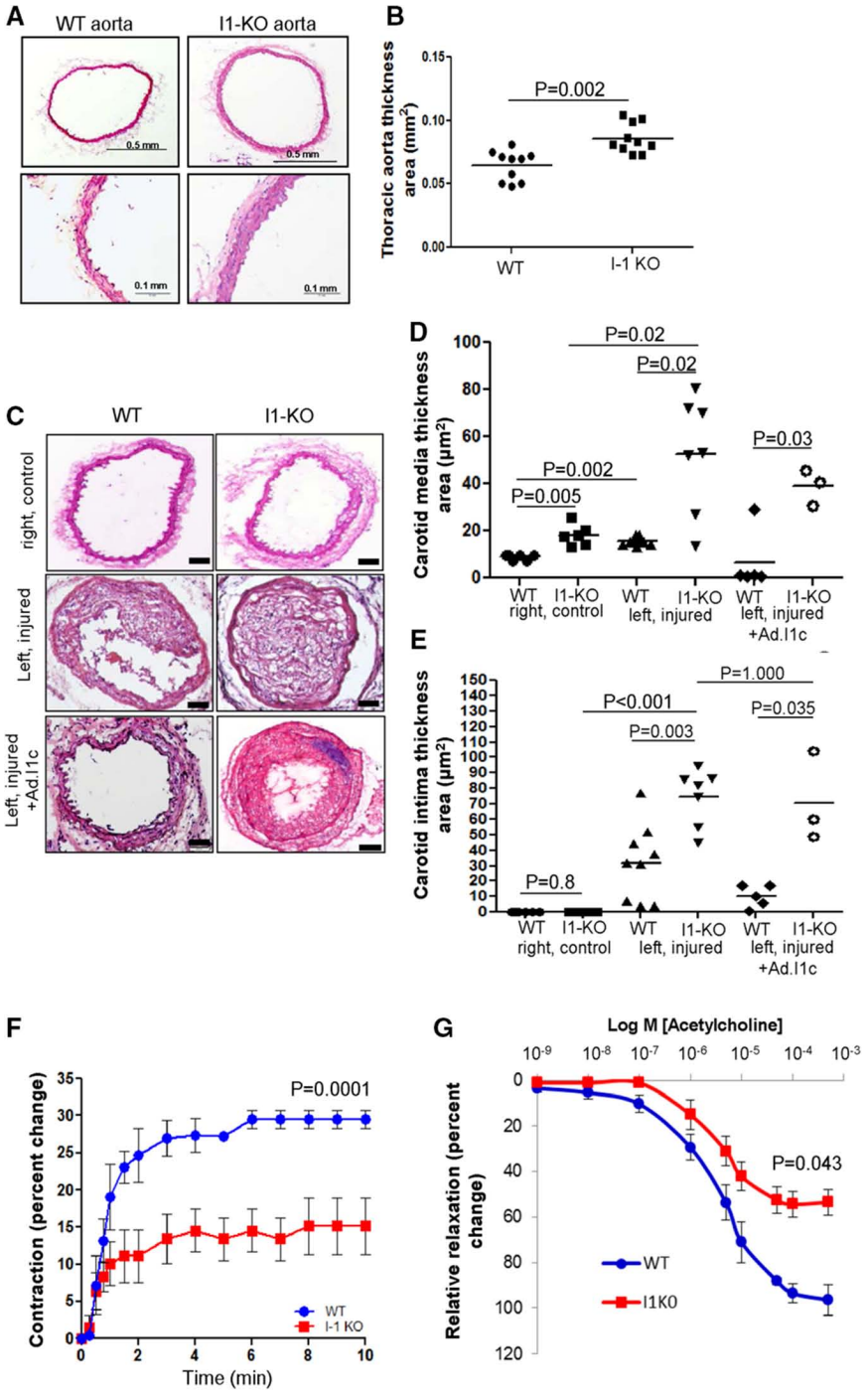

Figure 3. Enhanced proliferative capacity of aortic vascular smooth muscle cells (VSMCs) from inhibitor 1 knockout (I-1 KO) mice. **A**, Bright-field photomicrograph of vascular hyperplasia in the aorta of I-1 KO vs wild-type (WT) mice. **B**, Quantification of thoracic aortic thickness in WT (n=10) and I-1 KO (n=10) mice. **C**, Bright-field photomicrograph of cross sections harvested 1 month after injury and stained with hematoxylin and eosin from noninjured control arteries (sham group) of WT (n=6) and I-1 KO (n=6), noninfected left injured carotid of WT (n=9) and I-1 KO (n=7), and constitutively active I-1 infected with adenovirus (Ad.I-1c) (WT, n=5; I-1 KO, n=3). Scale bar, 50 μm. **D** and **E**, Dot plots showing morphometric measurements of media and intima thickness area, respectively, in control noninjured, injured nontransduced, and injured infected I-1c carotid arteries. **F**, Time-response curve for prostaglandin F2α (1 μmol/L) and (**G**) dose-response curve for acetylcholine-mediated relaxation of femoral arteries from WT (blue; n=3) and I-1 KO (red; n=5). Percent changes in vessel diameter were calculated by the difference from baseline. For relaxation, baseline was the precontraction state after administration of prostaglandin F2α (1 μmol/L). Values represent mean±SEM. The maximum strength of contraction and relaxation was significantly lower in I-1 KO.

Next, we analyzed the effect of I-1c expression on Ca^{2+} transients. Because in VSMCs the Ca^{2+} signal required for proliferation depends on both SR Ca^{2+} release and store operated Ca^{2+} entry (SOCE),[15] we performed Ca^{2+} transient recording in the absence of extracellular Ca^{2+} (EGTA). We have previously shown that during proliferation of VSMCs, the caffeine-induced Ca^{2+} transient, normally observed in contractile VSMCs, is progressively lost in favor of an inositol triphosphate–induced Ca^{2+} transient.[10] Here, we examined the inositol triphosphate–induced Ca^{2+} transients generated by agonist. In hCASMCs infected with Ad.β galactosiase (Ad.βGal), serum induced a long-lasting increase in cytosolic Ca^{2+} as a result of SR Ca^{2+} release (Figure 4C). The addition of Ca^{2+} to the extracellular medium triggered SOC in these cells (Figure 4C). Similar transients were observed in control noninfected cells (not shown). Surprisingly, I-1c expression had no effect on Ca^{2+} transients in synthetic hCASMCs (Figure 4D and Figure VIA–VID in the online-only Data Supplement). In line with this, the increase in PLB phosphorylation by I-1c expression (Figure 4A) had no effect on Ca^{2+}-ATPase activity because the overall store load was unchanged in I-1c–expressing cells compared with cells infected with control virus (Figure VIA in the online-only Data Supplement). Meanwhile, when cells were infected with an adenovirus encoding SERCA2a,

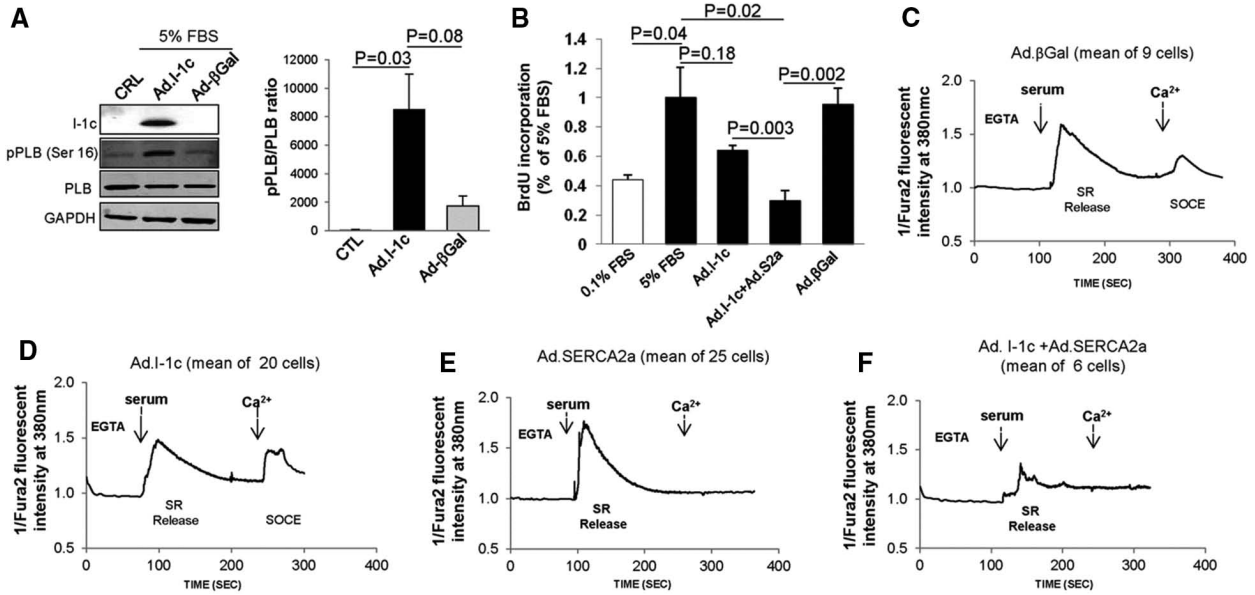

Figure 4. Effect of constitutively active inhibitor 1 (I-1c) overexpression on human coronary artery smooth muscle cells (hCASMCs). **A**, Immunoblot analysis (**left**) for indicated proteins and relative quantification of phospholamban phosphorylation (pPLB) expression (**right**) in hCASMCs infected with the indicated adenovirus. **B**, Effect of I-1c infected with adenovirus (Ad.I-1c), Ad.β galactosiase (Ad.βGal), and Ad.I-1c together with SERCA2a infected with adenovirus (Ad.SERCA2a) on hCASMC proliferation. Cells were infected with the aforementioned virus for 48 hours and then cultured for 48 hours in virus-free BrdU in 5% FBS medium. Bars represent the mean±SEM of BrdU incorporation of 4 independent experiments. Data are expressed as a percentage of control cells cultured in 5% FBS. Values represent mean±SEM. **C** through **F**, Analysis of I-1c overexpression on Ca^{2+} transients in synthetic hCASMCs. Intracellular Ca^{2+} imaging recorded in Fura-2–loaded cells representative of 3 experiments obtained from 3 independent infections. Cells were infected with Ad.βGal (**C**), Ad.I-1c (**D**), Ad.SERCA2a (**E**), or both Ad.I-1c and Ad.SERCA2a (**F**) for 2 days and then cultured for 24 hours in virus-free and serum-free medium before Ca^{2+} transient recording. Fluorescence intensity was recorded only in response to 1 excitation wavelength (380 nm). Traces represent the mean of several cells recordings. To record sarco/endoplasmic reticulum (SR) Ca^{2+} release and store operated Ca^{2+} entry (SOCE) activation, cells were treated with 5% serum buffered with EGTA in the absence of extracellular Ca^{2+} (EGTA, 100 μmol/L); extracellular Ca^{2+} ($CaCl_2$, 300 μmol/L) was then added at the indicated time.

SOC was not observed after Ca^{2+} addition to the extracellular medium (Figure 4E), confirming previous observations.[15] Remarkably, in cells coexpressing SERCA2a and I-1c, the serum-induced SR Ca^{2+} transient was significantly reduced, and SOC after the addition of Ca^{2+} to the extracellular medium was not observed (Figure 4F and Figure VIA-VID in the online-only Data Supplement). These data suggest that I-1c increased SERCA2a activity, that the type of Ca^{2+} transient is an SERCA2a isoform–dependent characteristic, and that the effects of I-1c and PLB phosphorylation on Ca^{2+} transients depend on SERCA2 isoform expression in VSMCs. When thapsigargin, a Ca^{2+}-mobilizing agent from SR, was added, the quantity of Ca^{2+} that was remobilized was higher in cells coexpressing SERCA2a and I-1c compared with βGal- and I-1c–expressing cells (Figure VIE and VIF in the online-only Data Supplement), demonstrating that I-1c and SERCA2a overexpression increased the SR Ca^{2+} load and Ca^{2+} uptake.

To validate the role of I-1 on PLB phosphorylation, CREB phosphorylated on Ser133, CREB responsive element, and NFAT activity through PP1, we performed siRNA knockdown to silence PP1 expression in hCASMCs. Immunoblot analysis of PP1 expression in hCASMCs cultured in 0.1% FBS for 4 days and transfected with pan PP1 or control siRNA showed that PP1 protein levels were decreased by 60% to 80% in PP1 siRNA-transfected hCASMCs (Figure VIIA in the online-only Data Supplement). CREB phosphorylation and PLB phosphorylation on Ser16 were increased in PP1 siRNA-transfected cells compared with controls (Figure VIIB in the online-only Data Supplement). CREB responsive element transcriptional activity was also significantly increased in PP1 siRNA-transfected cells compared with controls (Figure VIIC in the online-only Data Supplement). However, NFAT-driven luciferase activity was significantly decreased in PP1 siRNA-transfected cells compared with controls (Figure VIID in the online-only Data Supplement). These results demonstrate that I-1 through PP1 controls CREB and NFAT transcriptional activity. NFAT activity was also measured in contractile and synthetic VSMCs overexpressing I-1c. Furthermore, I-1c overexpression in contractile VSMCs significantly decreased NFAT activity compared with synthetic VSMCs. However, in cells coexpressing I-1c and SERCA2a, NFAT activity was significantly decreased in synthetic VSMCs. Infection with Ad.βGal had no effect on NFAT activity in either contractile or synthetic VSMCs (Figure VIIE in the online-only Data Supplement).

Effect of I-1 on Ca^{2+} Cycling and Signaling in Contractile and Synthetic Rat Aortic VSMCs

In the aforementioned adenovirus transduction experiments, we used a green fluorescent protein tag to identify infected cells. Because both viruses (Ad.SERCA2a and Ad.I-1c) were tagged with green fluorescent protein, we were unable to ascertain whether any given cell was infected with 1 or both viruses, even though the rate of infection for each virus was ≈80%. To avoid this uncertainty, we performed experiments using freshly dissociated contractile rat aortic VSMCs,

expressing SERCA2a, and synthetic cultured rat aortic VSMCs, expressing mainly SERCA2b.[11,14] The phenotypic status of the rat aortic VSMCs was verified by analyzing the expression of contractile proteins: smooth muscle α-actin, SM-MHC, and calponin (Figure VIIIA in the online-only Data Supplement). In parallel, the cyclin D1 protein level was increased in synthetic VSMCs (Figure VIIIA in the online-only Data Supplement). By immunostaining, cyclin D1 was not detected in freshly dissociated VSMCs, confirming their nonproliferative contractile phenotype. Three days after induction of proliferation by serum (10% FBS), cyclin D1 was expressed, demonstrating the proliferative synthetic phenotype (Figure VIIIB in the online-only Data Supplement). As expected, SERCA2a and I-1 were expressed in contractile VSMCs and downregulated in synthetic VSMCs (Figure 5A and Figure VIIIB in the online-only Data Supplement). p21 and p53 expression, CREB phosphorylated on Ser133, and PLB phosphorylation were also decreased in rat synthetic VSMCs (Figure 5A).

The initial Ca^{2+} event of VSMC dedifferentiation is the downregulation of Ca^{2+}-ATPase activity, which results in a sustained increase in cytosolic Ca^{2+} and increased calcineurin-NFAT activity.[11] Because I-1 downregulation is a part of the dedifferentiation process, we assessed the effect of I-1c overexpression on the dedifferentiation, proliferation, and Ca^{2+} transient of contractile VSMCs. Immediately after dissociation of rat aortic VSMCs, contractile aortic VSMCs were infected with Ad.I-1c or βGal virus and analyzed at day 4 after infection in a high concentration of FBS (10%). Remarkably, expression of I-1c prevented dedifferentiation of contractile VSMCs induced by serum, as attested by a sustained increase in SERCA2a and SM-MHC mRNA expression (Figure 5B). As expected, exposure to serum induced proliferation of contractile VSMCs, with the percentage of proliferation being similar to that in synthetic VSMCs (Figure 5C). Infection of VSMCs with Ad.I-1c significantly reduced proliferation of contractile VSMCs without any effect on synthetic VSMC proliferation (Figure 5C). Of note, infection of contractile VSMCs with Ad.βGal had no effect on VSMC proliferation or on serum-induced dedifferentiation (Figure 5B and 5C). Next, we examined Ca^{2+} transients in contractile and synthetic rat aortic VSMCs (Figure 5D–5I). As expected, thrombin induced SR Ca^{2+} release in contractile VSMCs with the inhibition of Ca^{2+} entry by SOCE after the addition of Ca^{2+} in the extracellular medium (Figure 5D). In contrast, in synthetic VSMCs, thrombin induced a large SR-released Ca^{2+} transient followed by SOC after the addition of Ca^{2+} (Figure 5E). Infection with control virus (Ad.βGal) had no effect on Ca^{2+} transients in either contractile or synthetic VSMCs (Figure 5F and 5G). Ad.I-1c overexpression had no effect on Ca^{2+} transients in synthetic rat VSMCs stimulated with serum compared with controls (Figure 5I and Figure IXB in the online-only Data Supplement) and in Ca^{2+} remobilized when thapsigargin was added (Figure IXC in the online-only Data Supplement), confirming the observations made for hCASMCs (Figure 4D). However, I-1c overexpression significantly decreased overall Ca^{2+} transients in contractile rat VSMCs stimulated with serum (Figure 5H and Figure IXA in the online-only Data Supplement), confirming that the effect of I-1 on Ca^{2+} transients depends on SERCA2a isoform expression in contractile versus synthetic VSMCs.

Constitutively Active I-1 Prevents Postinjury Remodeling and Neointimal Proliferation in a Rat Carotid Injury Model

Because I-1c overexpression prevents dedifferentiation and proliferation of contractile VSMCs in vitro, we next tested the possibility that I-1c gene transfer may prevent postangioplasty neointimal proliferation. For this purpose, we performed balloon injury in the left carotid arteries of adult male rats, followed immediately by gene transfer of Ad.I-1c or Ad.βGal. The right carotid was used as sham operated, noninjured. Animals were euthanized 2 weeks after injury, and neointimal thickening was analyzed on hematoxylin and eosin–stained cross sections (Figure 6A). Infection was confirmed by polymerase chain reaction detection of green fluorescent protein DNA in the carotid arteries infected with Ad.I-1c compared with noninfected arteries (Figure X in the online-only Data Supplement). Injury induced abundant neointimal proliferation and an increase in the medial thickness in noninfected (saline) or Ad.βGal-infected arteries, whereas infection with Ad.I-1c significantly reduced medial thickening and prevented neointimal proliferation (Figure 6B). Analysis by immunofluorescence microscopy confirmed that in saline- and Ad.βGal-infected arteries, there was downregulation of I-1 in the injured carotid segments, as well as downregulation of markers of the contractile phenotype such as SM-MHC and SERCA2a (Figure 7A). In contrast, in Ad.I-1c–infected arteries, I-1 expression was detected; however, our antibody does not allow us to discriminate between the endogenous and the transgene I-1 protein. Nevertheless, expression of SERCA2a and SM-MHC was preserved in I-1c–infected arteries (Figure 7A). In addition, the expression of CREB and p21 was lower in the media and adventitia of βGal-infected carotid arteries compared with arteries treated with Ad.I-1c. However, NFAT expression was highly increased in the βGal- compared with the I-1c–infected injured carotid (Figure 7B). Thus, I-1c prevented dedifferentiation and proliferation of contractile VSMCs expressing SERCA2a but had no effect on synthetic VSMCs, which predominantly express the SERCA2b isoform and NFATC3.

Discussion

The important finding of the present study is that PKA/I-1 downstream signaling pathways are organized differently in contractile and synthetic VSMCs (Figure 8). This signaling specificity is supported by altered expression of molecules involved in the regulation of the downstream of the cAMP/PKA signaling cascade, with I-1 and PP1 possibly providing of dual control of the signaling pathway at both the protein expression and phosphorylation levels. We demonstrated mirrored expression of I-1 and PP1 within contractile and synthetic VSMCs, leading to the enhancement of the PKA pathway in contractile VSMCs. I-1 is more highly expressed in the media of human coronary and freshly dispersed rat aortic VSMCs than in their cultured counterparts. The expression of I-1 correlated closely with the expression of genes for contractile proteins: smooth muscle α-actin (SMA), calponin, SERCA2a, and the

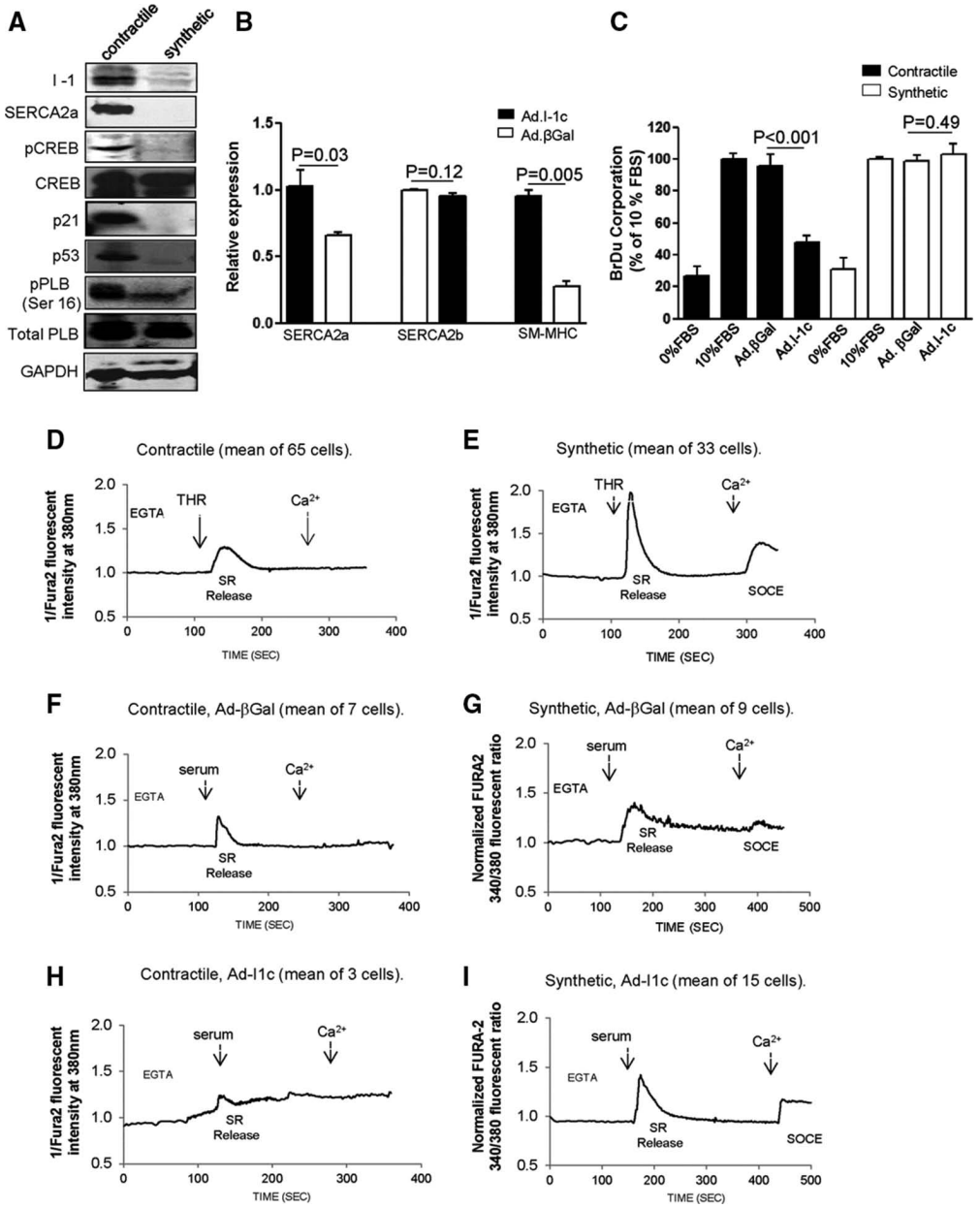

Figure 5. Effect of constitutively active inhibitor 1 (I-1c) expression on contractile and synthetic rat aortic vascular smooth muscle cells (VSMCs). **A**, Immunoblot analysis with the indicated proteins in contractile and synthetic aortic VSMCs from adult male rats. CREB indicates cAMP-responsive element binding; and p, phosphorylated. **B**, Real-time reverse transcription–polymerase chain reaction analysis showing the relative expression of sarco/endoplasmic reticulum calcium-ATPase (SERCA) 2a, SERCA2b, and smooth muscle myosin heavy chain (SM-MHC) in freshly dissociated contractile rat VSMCs infected with either constitutively active I-1 infected with adenovirus (Ad.I-1c) or Ad.β galactosiase (Ad.βGal). The cells were cultured in the presence of serum (10%) and were collected 4 days after infection. **C**, Effect of Ad.I-1c and Ad.βGal infection on proliferation of contractile and synthetic rat aortic VSMCs. Cells were infected with the aforementioned virus for 48 hours and then cultured for 48 hours in virus-free BrdU-containing medium supplemented with serum (10%). Bars represent the mean±SEM of BrdU incorporation of 4 independent experiments. Data are expressed as a percentage of control cells cultured in 10% serum. **D** and **E**, Analysis of Ca^{2+} transients in contractile and synthetic rat VSMCs. Representative intracellular Ca^{2+} imaging recorded in Fura-2–loaded cells from a total of 3 experiments obtained from 3 independent infections. Contractile cells were cultured without serum and used within 3 days after dissociation from the aorta. THR indicates thrombin. The cells were infected with Ad.βGal (**F** and **G**) or Ad.I-1c (**H** and **I**) for 2 days and then cultured for 24 hours in virus-free and serum-free medium before recording. Fluorescence intensity was only recorded in response to 1 excitation wavelength (380 nm). Traces represent the mean of several cells recordings. To record sarco/endoplasmic reticulum (SR) Ca^{2+} release and store operated Ca^{2+} entry (SOCE) activation, cells were treated with 5% serum buffered with EGTA (100 μmol/L) in the absence of extracellular Ca^{2+}; extracellular Ca^{2+} ($CaCl_2$; 300 μmol/L) was then added at the indicated time.

SM-MHC proteins, which are also downregulated in synthetic dedifferentiated VSMCs.[15] Therefore, these results establish a clear link between the differentiated, contractile phenotype of VSMCs and the downregulation of I-1 in rat and human VSMCs, suggesting a possible role for I-1 in the maintenance or function of the differentiated VSMC phenotype.

Moreover, we showed that VSMCs obtained from I-1KO mice are in a proliferative state and display the characteristics

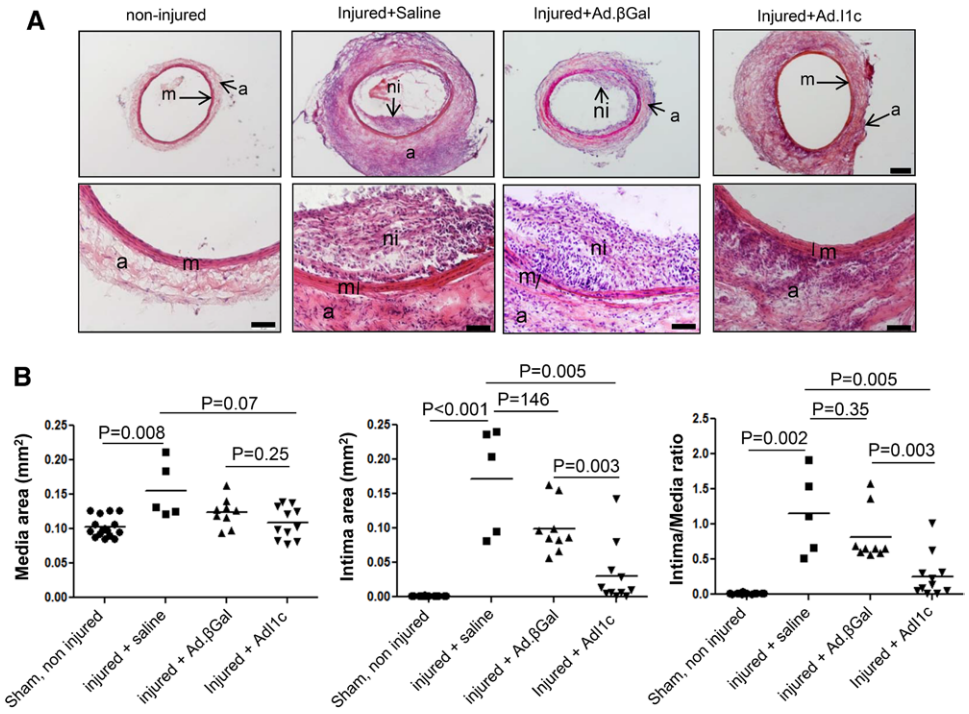

Figure 6. Constitutively active inhibitor 1 (I-1c) gene transfer prevents balloon angioplasty-associated restenosis in a rat carotid injury model. **A**, Bright-field photomicrograph of hematoxylin and eosin–stained cross sections from sham control (noninjured carotid, n=16) and injured treated saline (n=5), Ad.β galactosiase (Ad.βGal) (n=9), and Ad.I1c (n=11) arteries 14 days after surgery. ad Indicates adventitia; m, media; and ni, neointima. Scale bar, 200 μm (**top**) and 100 μm (**bottom**). **B**, Measurements of media and intima area size and intima/media area ratio of the 4 groups from **A**. Values represent mean±SEM.

of immature or dedifferentiated phenotypes compared with WT SMCs. I-1 KO VSMCs expressed minimal differentiation marker proteins such as smooth muscle α-actin and SM-MHC and showed an increase in proliferation markers such as cyclin D1 and proliferating cell nuclear antigen. More interestingly, in contrast to PP1, SERCA2a protein levels, together with PLB phosphorylation and therefore Ca^{2+}-ATPase, were reduced. However, when constitutively active I-1 is overexpressed, SERCA2a activity can be further increased. We also demonstrated that in vivo gene transfer of constitutively active I-1c prevents VSMC dedifferentiation and neointimal formation in a rat and mouse carotid injury model. However, in I-1 KO mice, because the VSMCs are dedifferentiated, neointimal formation was not decreased after I-1c overexpression. Thus, I-1 and SERCA2a are necessary and act synergistically to regulate the VSMC phenotype.

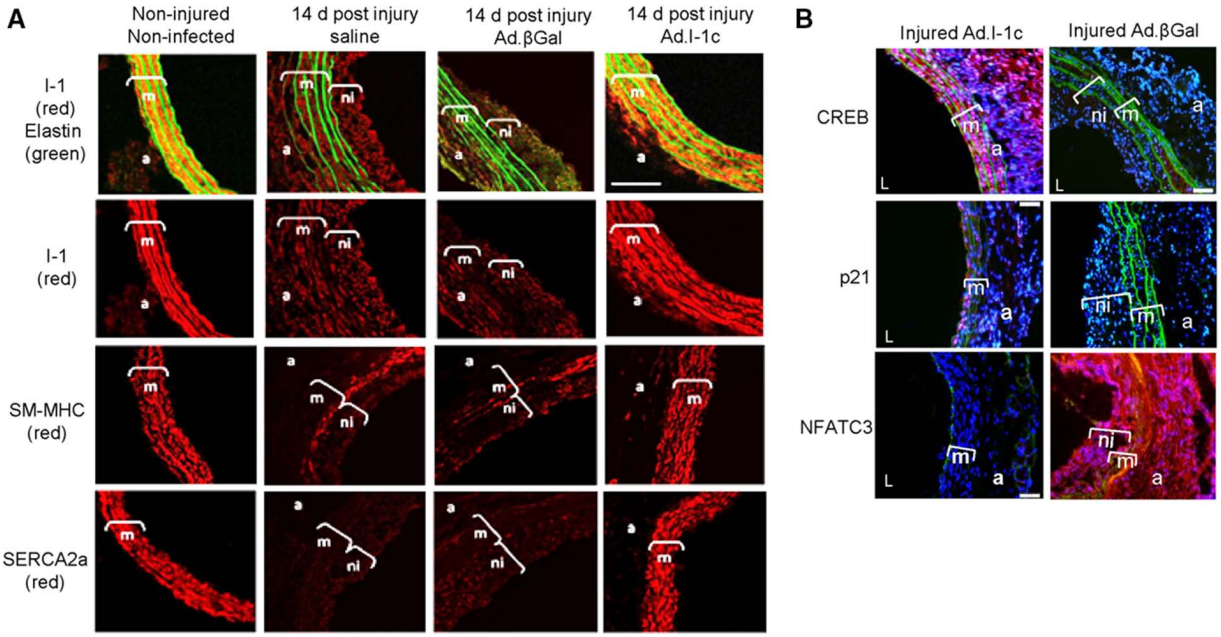

Figure 7. Constitutively active inhibitor 1 (I-1c) overexpression preserves the vascular smooth muscle cell (VSMC) contractile phenotype in balloon-injured rat carotid arteries. **A,** Immunolabeling of control or balloon-injured carotid arteries with anti–inhibitor 1 (I-1), anti–sarco/endoplasmic reticulum calcium-ATPase (SERCA) 2a, or anti–smooth muscle myosin heavy chain (SM-MHC; red). Elastin autofluorescence is shown in green. Bar scale, 20 μm. **B**, Representative cAMP-responsive element binding (CREB), p21, and nuclear factor of activated T cell (NFAT) C3 immunostaining of cross sections from βGal- and I-1c–infected arteries at 2 weeks after surgery. Red shows CREB-, p21-, and NFAT-positive staining. Ad.βGal indicates Ad.β galactosiase; a, adventitia; m, media; and ni, neointima.

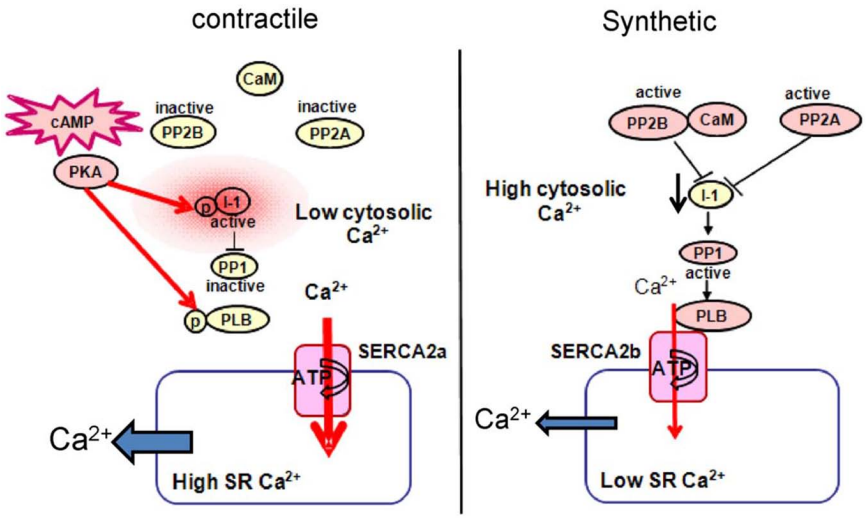

Figure 8. Schematic representation of protein kinase A (PKA)/inhibitor 1 (I-1)/protein phosphatase 1 (PP1) signaling pathways in contractile (**left**) and synthetic (**right**) vascular smooth muscle cells (VSMCs). CaM indicates calmodulin; p, phosphate; PLB, phospholamban; PP2A, protein phosphatase 2A; PP2B, protein phosphatase 2B; SERCA, sarco/endoplasmic reticulum Ca^{2+}-ATPase; and SR, sarco/endoplasmic reticulum.

A further interesting observation that can be drawn from the I-1 KO mice is the increase in aortic thickness resulting from hyperplasia and the excessive neointimal formation with vascular injury in vivo. The results presented here demonstrate that loss of I-1 in a mouse model increases SMC proliferation. These data support the hypothesis that a hyperplastic response modulated by I-1 in VSMCs contributes to vascular disease. In the heart, I-1 was found to be downregulated and hypophosphorylated in human and experimental heart failure but hyperactive in human atrial fibrillation, implicating I-1 in the pathogenesis of heart failure and arrhythmias.[34] In addition, constitutive I-1c expression by gene transfer restored contractile properties in failing rat hearts and failing human cardiac myocytes.[21,22] In our study, we showed that I-1c overexpression in carotid artery injury models prevented the downregulation of the expression of VSMC contractile markers such as SERCA2a and SM-MHC, as well as CREB and p21 expression. Several studies have also shown that downregulation of CREB expression or phosphorylation is associated with elevated cardiovascular risk markers in rodent models.[35] Indolfi et al[36] have reported that PKA signaling inhibits neointimal formation after vascular injury in vivo as a model of restenosis after angioplasty. In addition, cAMP signaling in SMCs has been shown to decrease the expression of cyclin D1[37] and to increase the expression of antiproliferative regulators like p53 and p21.[38] Furthermore, I-1c overexpression in contractile VSMCs also decreased transcription factor NFAT activity required for proliferation and migration of VSMCs that express SERCA2a.[13,15] We have shown that the restoration of SERCA2a expression by gene transfer in synthetic VSMCs was sufficient to block their proliferation and migration via inhibition of NFAT[15]; however, it will be interesting to assess whether SERCA2a gene transfer restores the I-1 expression level. The molecular mechanisms of this effect are related to the prevention of a functional association between STIM1 and OraI-1 (CRAC protein entity), which leads to the suppression of SOCE channel influx.[15] It is worth mentioning that SOC influx after agonist stimulation is not observed in contractile VSMCs, which express SERCA2a and I-1, compared with synthetic VSMCs. This suggests that I-1 exerts its effects through SERCA2a.

In addition, I-1 KO femoral arteries in vivo displayed a significantly lower vasoconstriction and vasorelaxation response compared with WT. These results suggest that changes in I-1 expression can modify the VSMC phenotype and therefore VSMC contractility. Indeed, the loss of I-1 in synthetic VSMCs and in the mouse model is associated with a reduced SR Ca^{2+}-ATPase activity. Therefore, I-1 is a critical determinant of SR Ca^{2+} uptake function. These results are particularly interesting when considered along with recent results demonstrating reduced endothelium-dependent relaxation in mice deficient in the SERCA3 isoform.[39] Another study showed that deletion of PLB can also reduce endothelium-dependent relaxation.[40] However, yet another study has suggested that ablation of I-1 does not play a major role in either tonic or phasic SM contractility in vivo. In that report, although I-1 did not have any major effects on the aorta, there was a significant, rightward-shifted (desensitized) response to isoproterenol in I-1 KO portal veins.[21] The difference between that study and our findings may potentially be attributable to the fact that our experiments were carried out in femoral arteries in vivo and the published study was done on mounted, isolated, denuded aortic rings.[21] In theory, the organization of the PKA/I-1 signaling pathway should increase SERCA2a activity in contractile VSMCs while inhibiting SERCA2a activity in synthetic cells. However, in reality, SERCA2a activity is further distinguished between contractile and synthetic VSMCs by SERCA2 isoform expression levels. In accordance with our previous observations,[10,14,15] we confirm here that the SERCA2a isoform is expressed exclusively in contractile VSMCs, whereas SERCA2b is the only SR Ca^{2+}-ATPase present in synthetic VSMCs. Furthermore, manipulation of these signaling pathways resulted in high SR Ca^{2+}-ATPase activity in contractile cells and reduced SR Ca^{2+}-ATPase activity in synthetic cells. In this case, we hypothesized that this reduction was attributable to enhanced endoplasmic reticulum Ca^{2+} uptake, leading to lower $[Ca]^{2+}_i$. Therefore, the interplay between Ca^{2+} release and uptake systems is an important determinant of endothelial steady-state Ca^{2+} levels that elicits endothelium-dependent relaxation.

Our study also shows that knockdown of PP1 enhances hyperphosphorylation of PLB and CREB and decreases

NFAT activity. Our results provide further evidence for a role of PP1 pathway in regulating the dephosphorylation of Ser133 and thereby limiting CREB transcriptional activity in synthetic VSMCs. Many studies have shown that increased PP1 activity is closely associated with the progression of heart failure.[16,22,41] PP1, a haloenzyme, consists of 3 distinct genes: *PP1c-alpha* (PP1α), *PP1c-gamma* (PP1λ), which gives rise to 2 splice variants (PP1c-λ1 and PP1c-λa2), and *PP1c-beta/delta* (PP1β),[42–44] the functions of which are not well characterized in cardiovascular cells. In our study, we found that PP1α and PP1β are increased in synthetic VSMCs. PP1β expression has been shown to gradually increase during the progressive time course of cardiac dysfunction in cardiomyopathic hamsters.[41] The expression levels of PP1β may have a crucial impact on SR Ca^{2+} cycling. The PP1β isoform was shown to be highly expressed in the longitudinal SR and formed a molecular complex with PLB and SERCA2a. Moreover, PP1β is the most significantly involved PP1 isoform in regulating PLB phosphorylation at Ser16 in the longitudinal SR, thereby controlling SR-mediated Ca^{2+} cycling in cardiomyocytes.[45]

Conclusions

We have demonstrated for the first time that Ca^{2+} signaling pathways via the I-1/PP1 signaling pathway are altered in synthetic VSMCs. I-1 expression appears to be a robust marker for contractile VSMCs, whereas PP1 expression is specific for synthetic VSMCs, thus reinforcing our finding of altered Ca^{2+} signaling. Furthermore, the synergistic action of I-1 and SERCA2a is necessary for the acquisition of high SERCA2a activity required for the contractile phenotype. Gene transfer of constitutive active I-1c to contractile VSMCs prevents injury-induced dedifferentiation and neointimal proliferations of VSMCs. Collectively, these data suggest that I-1c gene transfer may be considered as a therapeutic strategy for preventing vascular proliferative disorders.

Sources of Funding

This work was supported by the American Heart Association grant SDG 0930116 N (Dr Lipskaia); National Heart, Lung, and Blood Institute grants K01 HL1031176-01 (Dr Hadri), K08HL111330 (Dr Kovacic,), and R01 HL080498 and R01 HL083156 (Dr Hajjar); by the Association Française Contre les Myopathies (Dr Bobe); by AFM16442 (Drs Bobe, Lipskaia, Lopez, and Hajjar); and by MEC-FEDER (BFU2010-C02-01; Drs Bobe and Lopez). Dr Lopez was supported by a postdoctoral fellowship from the Junta de Extremadura (POS0922).

Disclosures

Dr Hajjar is a scientific founder of Celladon Corp, which plans to commercialize AAV1.SERCA2a for the treatment of heart failure. The other authors report no conflicts.

References

1. Novak K. Cardiovascular disease increasing in developing countries. *Nat Med*. 1998;4:989–990.
2. Dzau VJ, Braun-Dullaeus RC, Sedding DG. Vascular proliferation and atherosclerosis: new perspectives and therapeutic strategies. *Nat Med*. 2002;8:1249–1256.
3. Forrester JS, Fishbein M, Helfant R, Fagin J. A paradigm for restenosis based on cell biology: clues for the development of new preventive therapies. *J Am Coll Cardiol*. 1991;17:758–769.
4. Braun-Dullaeus RC, Mann MJ, Dzau VJ. Cell cycle progression: new therapeutic target for vascular proliferative disease. *Circulation*. 1998;98:82–89.
5. Chen KH, Guo X, Ma D, Guo Y, Li Q, Yang D, Li P, Qiu X, Wen S, Xiao RP, Tang J. Dysregulation of HSG triggers vascular proliferative disorders. *Nat Cell Biol*. 2004;6:872–883.
6. Marchand A, Abi-Gerges A, Saliba Y, Merlet E, Lompré AM. Calcium signaling in vascular smooth muscle cells: from physiology to pathology. *Adv Exp Med Biol*. 2012;740:795–810.
7. Regan CP, Adam PJ, Madsen CS, Owens GK. Molecular mechanisms of decreased smooth muscle differentiation marker expression after vascular injury. *J Clin Invest*. 2000;106:1139–1147.
8. House SJ, Potier M, Bisaillon J, Singer HA, Trebak M. The non-excitable smooth muscle: calcium signaling and phenotypic switching during vascular disease. *Pflugers Arch*. 2008;456:769–785.
9. Golovina VA, Platoshyn O, Bailey CL, Wang J, Limsuwan A, Sweeney M, Rubin LJ, Yuan JX. Upregulated TRP and enhanced capacitative Ca(2+) entry in human pulmonary artery myocytes during proliferation. *Am J Physiol Heart Circ Physiol*. 2001;280:H746–H755.
10. Vallot O, Combettes L, Jourdon P, Inamo J, Marty I, Claret M, Lompré AM. Intracellular Ca(2+) handling in vascular smooth muscle cells is affected by proliferation. *Arterioscler Thromb Vasc Biol*. 2000;20:1225–1235.
11. Lipskaia L, Pourci ML, Deloménie C, Combettes L, Goudounèche D, Paul JL, Capiod T, Lompré AM. Phosphatidylinositol 3-kinase and calcium-activated transcription pathways are required for VLDL-induced smooth muscle cell proliferation. *Circ Res*. 2003;92:1115–1122.
12. Gomez MF, Stevenson AS, Bonev AD, Hill-Eubanks DC, Nelson MT. Opposing actions of inositol 1,4,5-trisphosphate and ryanodine receptors on nuclear factor of activated T-cells regulation in smooth muscle. *J Biol Chem*. 2002;277:37756–37764.
13. Dolmetsch RE, Lewis RS, Goodnow CC, Healy JI. Differential activation of transcription factors induced by Ca^{2+} response amplitude and duration. *Nature*. 1997;386:855–858.
14. Lipskaia L, del Monte F, Capiod T, Yacoubi S, Hadri L, Hours M, Hajjar RJ, Lompré AM. Sarco/endoplasmic reticulum Ca^{2+}-ATPase gene transfer reduces vascular smooth muscle cell proliferation and neointima formation in the rat. *Circ Res*. 2005;97:488–495.
15. Bobe R, Hadri L, Lopez JJ, Sassi Y, Atassi F, Karakikes I, Liang L, Limon I, Lompré AM, Hatem SN, Hajjar RJ, Lipskaia L. SERCA2a controls the mode of agonist-induced intracellular Ca2+ signal, transcription factor NFAT and proliferation in human vascular smooth muscle cells. *J Mol Cell Cardiol*. 2011;50:621–633.
16. Nicolaou P, Kranias EG. Role of PP1 in the regulation of Ca cycling in cardiac physiology and pathophysiology. *Front Biosci (Landmark Ed)*. 2009;14:3571–3585.
17. El-Armouche A, Rau T, Zolk O, Ditz D, Pamminger T, Zimmermann WH, Jäckel E, Harding SE, Boknik P, Neumann J, Eschenhagen T. Evidence for protein phosphatase inhibitor-1 playing an amplifier role in beta-adrenergic signaling in cardiac myocytes. *FASEB J*. 2003;17:437–439.
18. Aitken A, Cohen P. Isolation and characterisation of active fragments of protein phosphatase inhibitor-1 from rabbit skeletal muscle. *FEBS Lett*. 1982;147:54–58.
19. Oliver CJ, Shenolikar S. Physiologic importance of protein phosphatase inhibitors. *Front Biosci*. 1998;3:D961–D972.
20. Tokui T, Brozovich F, Ando S, Ikebe M. Enhancement of smooth muscle contraction with protein phosphatase inhibitor 1: activation of inhibitor 1 by cGMP-dependent protein kinase. *Biochem Biophys Res Commun*. 1996;220:777–783.
21. Carr AN, Schmidt AG, Suzuki Y, del Monte F, Sato Y, Lanner C, Breeden K, Jing SL, Allen PB, Greengard P, Yatani A, Hoit BD, Grupp IL, Hajjar RJ, DePaoli-Roach AA, Kranias EG. Type 1 phosphatase, a negative regulator of cardiac function. *Mol Cell Biol*. 2002;22:4124–4135.
22. Pathak A, del Monte F, Zhao W, Schultz JE, Lorenz JN, Bodi I, Weiser D, Hahn H, Carr AN, Syed F, Mavila N, Jha L, Qian J, Marreez Y, Chen G, McGraw DW, Heist EK, Guerrero JL, DePaoli-Roach AA, Hajjar RJ, Kranias EG. Enhancement of cardiac function and suppression of heart failure progression by inhibition of protein phosphatase 1. *Circ Res*. 2005;96:756–766.
23. Mulkey RM, Endo S, Shenolikar S, Malenka RC. Involvement of a calcineurin/inhibitor-1 phosphatase cascade in hippocampal long-term depression. *Nature*. 1994;369:486–488.
24. El-Armouche A, Bednorz A, Pamminger T, Ditz D, Didié M, Dobrev D, Eschenhagen T. Role of calcineurin and protein phosphatase-2A in the regulation of phosphatase inhibitor-1 in cardiac myocytes. *Biochem Biophys Res Commun*. 2006;346:700–706.

25. Braz JC, Gregory K, Pathak A, Zhao W, Sahin B, Klevitsky R, Kimball TF, Lorenz JN, Nairn AC, Liggett SB, Bodi I, Wang S, Schwartz A, Lakatta EG, DePaoli-Roach AA, Robbins J, Hewett TE, Bibb JA, Westfall MV, Kranias EG, Molkentin JD. PKC-alpha regulates cardiac contractility and propensity toward heart failure. *Nat Med*. 2004;10:248–254.
26. Rodriguez P, Mitton B, Waggoner JR, Kranias EG. Identification of a novel phosphorylation site in protein phosphatase inhibitor-1 as a negative regulator of cardiac function. *J Biol Chem*. 2006;281:38599–38608.
27. Rodriguez P, Mitton B, Nicolaou P, Chen G, Kranias EG. Phosphorylation of human inhibitor-1 at Ser67 and/or Thr75 attenuates stimulatory effects of protein kinase A signaling in cardiac myocytes. *Am J Physiol Heart Circ Physiol*. 2007;293:H762–H769.
28. Somlyo AP, Somlyo AV. Signal transduction by G-proteins, rho-kinase and protein phosphatase to smooth muscle and non-muscle myosin II. *J Physiol*. 2000;522(pt 2):177–185.
29. Elbrecht A, DiRenzo J, Smith RG, Shenolikar S. Molecular cloning of protein phosphatase inhibitor-1 and its expression in rat and rabbit tissues. *J Biol Chem*. 1990;265:13415–13418.
30. Alessi D, MacDougall LK, Sola MM, Ikebe M, Cohen P. The control of protein phosphatase-1 by targetting subunits: the major myosin phosphatase in avian smooth muscle is a novel form of protein phosphatase-1. *Eur J Biochem*. 1992;210:1023–1035.
31. Allen PB, Hvalby O, Jensen V, Errington ML, Ramsay M, Chaudhry FA, Bliss TV, Storm-Mathisen J, Morris RG, Andersen P, Greengard P. Protein phosphatase-1 regulation in the induction of long-term potentiation: heterogeneous molecular mechanisms. *J Neurosci*. 2000;20:3537–3543.
32. Tang EH, Jensen BL, Skott O, Leung GP, Feletou M, Man RY, Vanhoutte PM. The role of prostaglandin E and thromboxane-prostanoid receptors in the response to prostaglandin E2 in the aorta of Wistar Kyoto rats and spontaneously hypertensive rats. *Cardiovasc Res*. 2008;78:130–138.
33. Dolmetsch RE, Pajvani U, Fife K, Spotts JM, Greenberg ME. Signaling to the nucleus by an L-type calcium channel-calmodulin complex through the MAP kinase pathway. *Science*. 2001;294:333–339.
34. Wittköpper K, Dobrev D, Eschenhagen T, El-Armouche A. Phosphatase-1 inhibitor-1 in physiological and pathological β-adrenoceptor signalling. *Cardiovasc Res*. 2011;91:392–401.
35. Schauer IE, Knaub LA, Lloyd M, Watson PA, Gliwa C, Lewis KE, Chait A, Klemm DJ, Gunter JM, Bouchard R, McDonald TO, O'Brien KD, Reusch JE. CREB downregulation in vascular disease: a common response to cardiovascular risk. *Arterioscler Thromb Vasc Biol*. 2010;30:733–741.
36. Indolfi C, Avvedimento EV, Di Lorenzo E, Esposito G, Rapacciuolo A, Giuliano P, Grieco D, Cavuto L, Stingone AM, Ciullo I, Condorelli G, Chiariello M. Activation of cAMP-PKA signaling in vivo inhibits smooth muscle cell proliferation induced by vascular injury. *Nat Med*. 1997;3:775–779.
37. Vadiveloo PK, Filonzi EL, Stanton HR, Hamilton JA. G1 phase arrest of human smooth muscle cells by heparin, IL-4 and cAMP is linked to repression of cyclin D1 and cdk2. *Atherosclerosis*. 1997;133:61–69.
38. Hayashi S, Morishita R, Matsushita H, Nakagami H, Taniyama Y, Nakamura T, Aoki M, Yamamoto K, Higaki J, Ogihara T. Cyclic AMP inhibited proliferation of human aortic vascular smooth muscle cells, accompanied by induction of p53 and p21. *Hypertension*. 2000;35(pt 2):237–243.
39. Liu LH, Paul RJ, Sutliff RL, Miller ML, Lorenz JN, Pun RY, Duffy JJ, Doetschman T, Kimura Y, MacLennan DH, Hoying JB, Shull GE. Defective endothelium-dependent relaxation of vascular smooth muscle and endothelial cell Ca^{2+} signaling in mice lacking sarco(endo)plasmic reticulum Ca^{2+}-ATPase isoform 3. *J Biol Chem*. 1997;272:30538–30545.
40. Sutliff RL, Hoying JB, Kadambi VJ, Kranias EG, Paul RJ. Phospholamban is present in endothelial cells and modulates endothelium-dependent relaxation: evidence from phospholamban gene-ablated mice. *Circ Res*. 1999;84:360–364.
41. Yamada M, Ikeda Y, Yano M, Yoshimura K, Nishino S, Aoyama H, Wang L, Aoki H, Matsuzaki M. Inhibition of protein phosphatase 1 by inhibitor-2 gene delivery ameliorates heart failure progression in genetic cardiomyopathy. *FASEB J*. 2006;20:1197–1199.
42. Cohen P, Alemany S, Hemmings BA, Resink TJ, Strålfors P, Tung HY. Protein phosphatase-1 and protein phosphatase-2A from rabbit skeletal muscle. *Methods Enzymol*. 1988;159:390–408.
43. Sasaki K, Shima H, Kitagawa Y, Irino S, Sugimura T, Nagao M. Identification of members of the protein phosphatase 1 gene family in the rat and enhanced expression of protein phosphatase 1 alpha gene in rat hepatocellular carcinomas. *Jpn J Cancer Res*. 1990;81:1272–1280.
44. Dombrádi V, Axton JM, Brewis ND, da Cruz e Silva EF, Alphey L, Cohen PT. Drosophila contains three genes that encode distinct isoforms of protein phosphatase 1. *Eur J Biochem*. 1990;194:739–745.
45. Aoyama H, Ikeda Y, Miyazaki Y, Yoshimura K, Nishino S, Yamamoto T, Yano M, Inui M, Aoki H, Matsuzaki M. Isoform-specific roles of protein phosphatase 1 catalytic subunits in sarcoplasmic reticulum-mediated Ca(2+) cycling. *Cardiovasc Res*. 2011;89:79–88.

CLINICAL PERSPECTIVE

Phenotypic switching of vascular smooth muscle cells (VSMCs) from a contractile/quiescent to a proliferative/synthetic phenotype plays a key role in vascular proliferative syndromes such as atherosclerosis and restenosis. VSMC phenotype switch is associated with alterations of VSMC Ca^{2+} handling proteins. Recently, we demonstrated that Ca^{2+} cycling in contractile VSMCs requires the expression of the sarco/endoplasmic reticulum Ca^{2+}-ATPase (SERCA) isoform SERCA2a. Protein phosphatase inhibitor-1 (I-1), a highly specific inhibitor of protein phosphatase 1, enhances protein kinase A–dependent phospholamban phosphorylation and therefore SERCA2a activity. In the present study, we examined the role of I-1 in the VSMC phenotype switch and the therapeutic potential of constitutively active I-1 (I1c) gene transfer in a postangioplasty restenosis model. In human coronary arteries, we showed that I-1 expression is specific to contractile VSMCs; however, in synthetic VSMCs, I-1 expression was significantly decreased, leading to an increase in its target PP1 and a decrease in phospholamban phosphorylation and SERCA2 activity. In cells coexpressing I-1c and SERCA2a, VSMC proliferation was decreased with an increase in Ca^{2+} uptake and sarco/endoplasmic reticulum Ca^{2+} load. I-1 knockout mice lack phospholamban phosphorylation and exhibit VSMC arrest in the synthetic state, with a significant modification of contractile properties and relaxant response of femoral artery in vivo and an excessive neointimal proliferation after carotid injury. Local I-1c gene transfer in a rat model of carotid injury decreased neointimal formation by preserving VSMC contractile marker expression and therefore preventing VSMC phenotypic switch. Gene transfer of I1c may be considered a therapeutic strategy for preventing vascular proliferative disorders.

Synergistic Role of Protein Phosphatase Inhibitor 1 and Sarco/Endoplasmic Reticulum Ca^{2+}-ATPase in the Acquisition of the Contractile Phenotype of Arterial Smooth Muscle Cells

Larissa Lipskaia, Regis Bobe, Jiqiu Chen, Irene C. Turnbull, Jose J. Lopez, Elise Merlet, Dongtaq Jeong, Ioannis Karakikes, Alexandra S. Ross, Lifan Liang, Nathalie Mougenot, Fabrice Atassi, Anne-Marie Lompré, Sima T. Tarzami, Jason C. Kovacic, Evangelia Kranias, Roger J. Hajjar and Lahouaria Hadri

Circulation. 2014;129:773-785; originally published online November 18, 2013;
doi: 10.1161/CIRCULATIONAHA.113.002565
Circulation is published by the American Heart Association, 7272 Greenville Avenue, Dallas, TX 75231

Print ISSN: 0009-7322. Online ISSN: 1524-4539

SUPPLEMENTAL MATERIAL

Materials. The following primary antibodies were used: anti-SERCA2a (21st Century Biochemicals, Marlborough, MA) and anti-SERCA2b [1], anti- non-muscular myosin heavy chain B (NM-B) (Ab 684, Abcam), anti-smooth muscle α actin cell (A5228, sigma), anti-smooth muscle myosin heavy chain (SM-MHC) (ab683, Abcam), anti-Cyclin D1 (556470, BD Biosciences), anti-h-calponin (C2687, Sigma-Aldrich), a-Cip1/WAF-1/p21 (2947, Cell Signaling), anti-glyceraldehyde 3-phosphate dehydrogenase (GAPDH) (G 8795, Sigma), anti-PLB (A010-14, Badrilla Ltd), anti-phospho Ser16 PLB (A010-12 Badrilla Ltd), anti-I1 (generously provided by Dr Kranias, University of Cincinnati), PCNA (sc-7907, Santa Cruz biotechnology, inc.), anti-CREB (06-86, Millipore), anti-p53 (9282, Cell Signaling), and pan PP1 (sc-7482, Santa Cruz biotechnology, inc.), anti-PP1α (sc-271762, Santa Cruz biotechnology, inc.), anti-PP1β (sc-373782, Santa Cruz biotechnology, inc.).

Adenovirus. The AdEasy XL Adenoviral Vector System (Stratagene) was used to generate recombinant adenoviral vectors. The following adenoviruses were used: Ad.S2a, encoding human SERCA2a and green fluorescence protein (GFP) under the cytomegalovirus (CMV) promoter [2]; Ad.βGal, encoding β-Galactosidase and GFP under the CMV promoter [2], and Ad.I-1c encoding constitutive active I-1 protein (I1c) and green fluorescent protein (GFP) under the CMV promoter. Optimized constitutively active form of I-1(I1c) cDNAs (201 bps in size) was subcloned into the pShuttle-IRES-hrGFP1 vector using NotI and SalI restriction enzymes.

Culture of VSMCs. Human Coronary Artery Smooth Muscle Cells (hCASMCs) were purchased from Lonza. Cells were cultured in SmBM medium (Lonza), containing Fetal bovine Serum (FBS) 5% and bullet kit (Lonza), at 5% of CO_2.

Rat aortic VSMCs were isolated from the media of the thoracic aorta of male sprague dawley rats by enzymatic digestion and cultured as described before[3]. Rat VSMCs were cultured in DMEM medium supplemented with Fetal Calf Serum (FCS) (10%) and 1% Penicillin-Streptomycin (Life Technology) at 5% of $C0_2$. VSMCs were used between passages 2 to 8 at 80% confluence. Cells were infected with adenovirus (100 MOI/cell) for 2 days and the efficiency of infection was controlled by GFP fluorescence. Proliferation was measured by BrdU incorporation during 48 hours using a Cell Proliferation ELISA, BrdU (colorimetric) assay kit (Roche) according to the manufacturer's instructions.

Cell viability assays. Cell viability was estimated using a fluorescent based Live/Dead Assay kit (Invitrogen) according to the manufacturer's instructions. The number of dead cells was estimated by flow cytometry using a FACScalibur flow cytometer equipped with CellQuestPro software (BD Biosciences). Data were collected with the Cellquest software (Becton Dickinson, Mansfield, USA).

Immunoblot analysis. Total cell lysates were separated by SDS-PAGE to perform Western blot analysis. Proteins were visualized by using the SuperSignal West Pico Chemiluminescent Substrate (Pierce Biotechnology).

Measure of SR Ca^{2+}-ATPase activity in VSMCs. Ca^{2+}-ATPase activity of SERCA2a activity was determined in SR microsomes using High Throughput Colorimetric ATPase Assays according to the manufacturer's instructions (Innova Biosciences). All assays were performed in triplicate.

RNA quantification. Total RNA was isolated using TRIzol reagent (Invitrogen) followed by a cleanup step as described in the RNeasy Isolation kit (Qiagen) with on-column DNase I

treatment to eliminate contaminating genomic DNA with an RNase-free DNase Set (Qiagen). About 1 μg of total RNA from each sample was reverse transcribed using the High Capacity cDNA Reverse Transcription kit (Applied Biosystems, ABI) according to the manufacturer's protocol. PCR reactions were performed with PCR Master Mix (Gibco), the following primers were used; human GFP forward: TGGTGAGCAAGCAGATCCTGAAGA, reverse: 5'-CTCCATGGTGAACACGTGGTTGTT-3'; human β-actin forward: CACCATTGGCAATGAGCGGTTC, reverse: 5'- AGGTCTTTGCGGATGTCCACGT-3'.

PP1 siRNA transfection . hCASMCs were transfected with pan PP1 siRNA (sc-43545 Santa Cruz Biotechnologies) and scramble siRNA (sc- sc-37007, Santa Cruz Biotechnologies) for 72 hours, using Lipofectamine 2000 (Invitrogen) according to the manufacturer's protocol.

CRE and NFAT-reporter gene assay. hCASMCs were cultured in 0.1% FBS and transfected with siRNA for 72 hours. The transfected cells were then infected with an adenovirus expressing CRE and NFAT-promoter-luciferase construct for 24 hours. The luciferase activity was measured using the Luciferase Assay System (Promega), normalized to total protein, and expressed as percent of control non-infected cells in relative luciferase units (RLU).

Mice Carotid Injury. C57BL/6J male mice weighing 28~35 g were used in these experiments. The animals were anesthetized by intraperitoneal injection with a solution composed of ketamine 65mg/Kg and xylazine 13 mg/Kg body weight diluted in 0.9% sodium chloride solution. The left common carotid artery was exposed via a midline incision on the ventral side of the neck. The bifurcation of the carotid artery was identified and two silk sutures were placed around the external carotid and the distal one was tied. Two temporary sutures were placed around the internal and common carotid arteries. An incision hole was made on the external carotid artery. A

curved wire (0.35 mm diameter) was introduced into the common carotid artery via the incision and the wire was passed along the vessel 3 times. The wire was then removed and the virus (Ad.I-1c) was infused in the artery for 30 min under pressure. Perfusion was restored through the internal and the common carotid artery after 30 minutes and the external carotid artery were tied off proximal to the incision with the proximal ligature. The sutures on internal and common carotid artery were released[4]. The right carotid was used as sham-operated (no wire injury).

Rat carotid artery injury and gene delivery. The left external carotid artery from adult male Sprague-Dawley rats (Charles River, Mass) weighing 350 to 400 g was injured using a 2F Fogarty embolectomy catheter (Baxter Healthcare Corp) that was introduced into the common carotid artery through the external carotid and inflated to 2 atmospheres three consecutive times, each inflation lasting for 20 seconds. Afterwards both the common and the internal carotid arteries were clamped on the proximal site. A viral infusion mixture containing $1x10^{11}$ pfu of virus vectors, diluted to a total volume of 100 µL was instilled between the 2 clamps, and the external carotid artery was then ligated. The virus infusion was maintained in the artery for 30 min under pressure. Perfusion was restored through the internal and the common carotid artery after 30 minutes of instillation, and the neck incision was closed. Fourteen days after surgery the animals were sacrificed. The left injured and right carotid arteries (used as sham-operated, non-injured) were dissected, flushed with saline solution, embedded in OCT and frozen at –80°C. A small piece from the middle portion was frozen in liquid nitrogen for eventual PCR analysis.

Histological analysis. The morphology of the aorta and carotid arteries was analyzed on hematoxylin/eosin stained cross-sections. The medial and neointimal areas were measured with a computer-based morphometric system (cellSens Entry software, Olympus) and calculated using Image J software. For each vessel, 5 discontinuous sections were analyzed.

Confocal microscopy. Immunocytochemistry was performed on acetone-fixed sections according to a standard protocol. Slides were examined with a Leica TCS4D confocal scanning laser microscope. Stacks of images were collected every 0.4 μm along the z-axis.

Supplemental References

1. Eggermont JA, Wuytack F, Verbist J, Casteels R. Expression of endoplasmic-reticulum ca2(+)-pump isoforms and of phospholamban in pig smooth-muscle tissues. *Biochem J*. 1990;271:649-653
2. del Monte F, Harding SE, Schmidt U, Matsui T, Kang ZB, Dec GW, Gwathmey JK, Rosenzweig A, Hajjar RJ. Restoration of contractile function in isolated cardiomyocytes from failing human hearts by gene transfer of serca2a. *Circulation*. 1999;100:2308-2311
3. Lipskaia L, del Monte F, Capiod T, Yacoubi S, Hadri L, Hours M, Hajjar RJ, Lompre AM. Sarco/endoplasmic reticulum ca2+-atpase gene transfer reduces vascular smooth muscle cell proliferation and neointima formation in the rat. *Circ Res*. 2005;97:488-495
4. Lindner V, Fingerle J, Reidy MA. Mouse model of arterial injury. *Circulation research*. 1993;73:792-796.

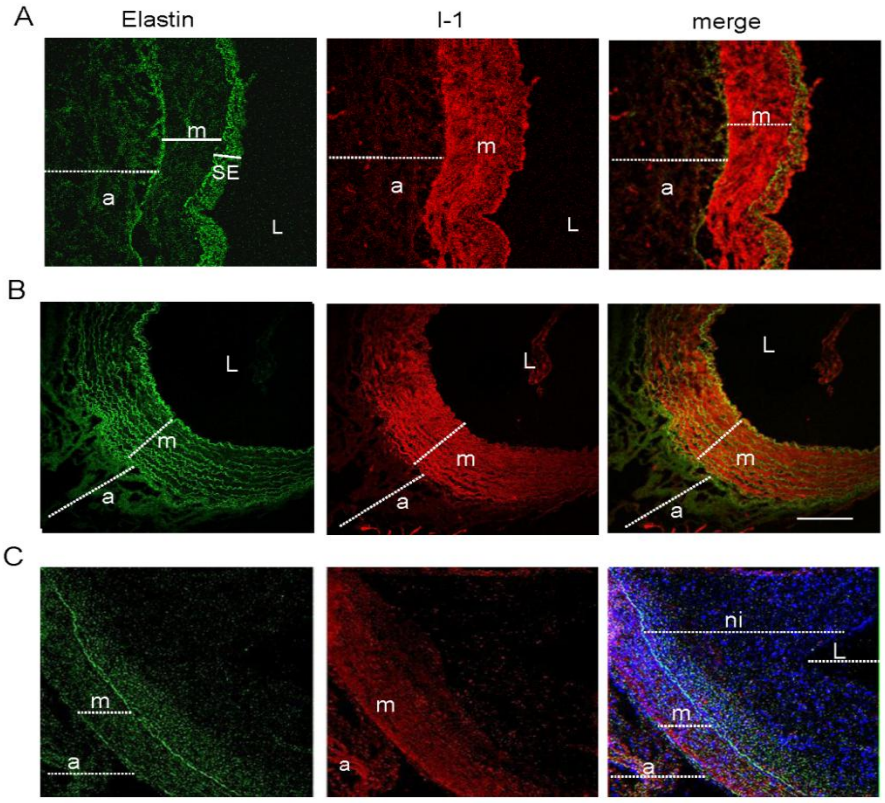

Supplementary Figure 1. (**A**) I-1expression (red) in human coronary artery (**B**) in internal mammary artery and (**C**) in atherosclerotic coronary artery by Confocal immunofluorescence microscopy. Elastin autofluorescence (green); a (adventitia); m (media), L (lumen).

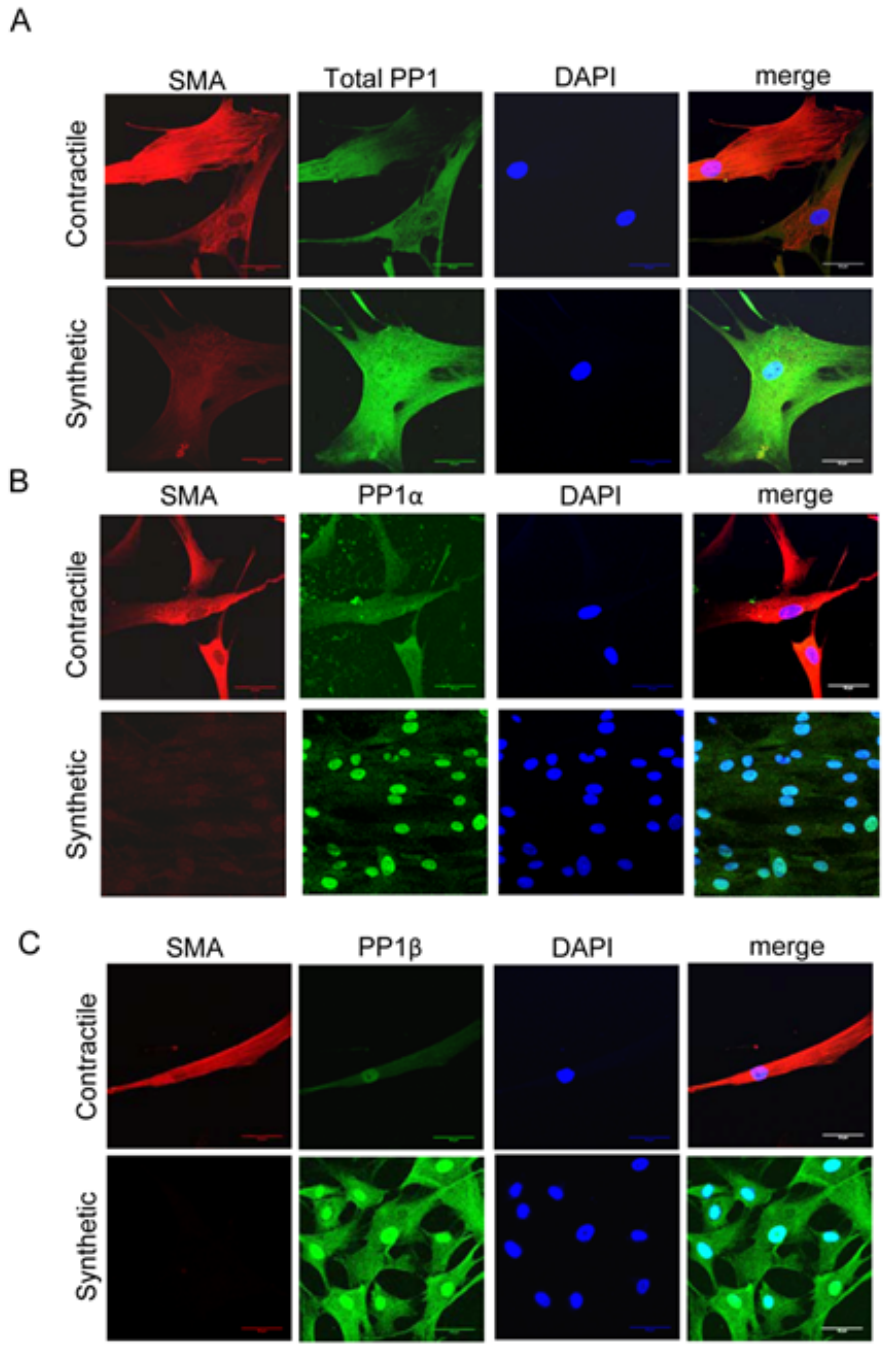

Supplementary Figure 2. Subcellular localization of PP1 isoform in contractile and synthetic human coronary artery smooth muscle cells (hCASMCS). (**A**) Contractile and synthetic hCAMSCs were co-immunostained using anti-total PP1 antibody (green) and anti-SMA (red). (**B**) hCASMCs were immunostained with anti-PP1α (green) and (**C**) with anti-PP1β (green). Bar Scale 50μm.

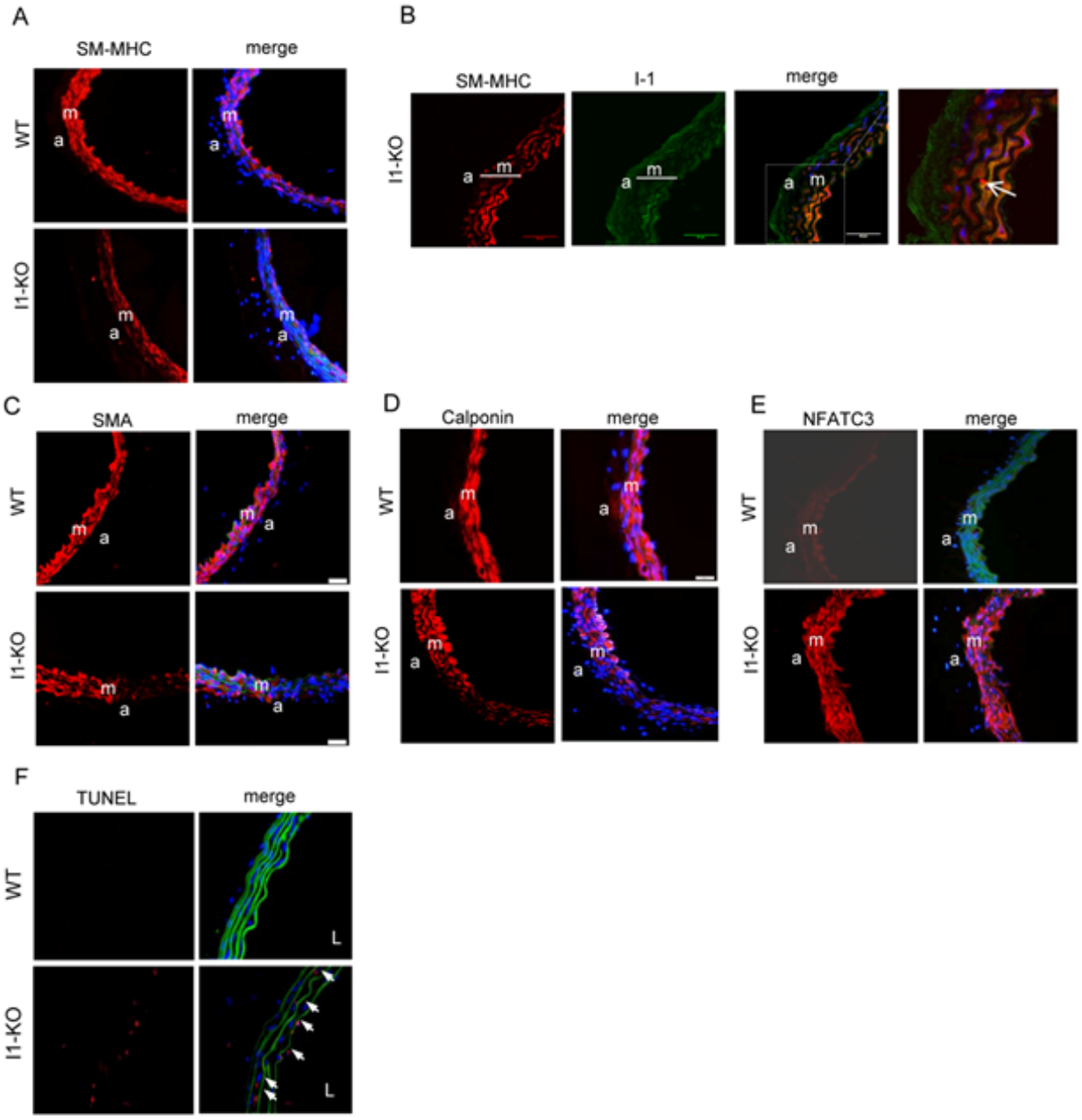

Supplementary Figure 3. **Immunostaining of VSMC protein markers in I-1 KO and WT aorta. (A**) VSMCs were stained with anti-SM-MHC (red). (**B**) Cells were co-stained with anti-SMMHC (red) and I-1 (green) and the images were merged (yellow) as indicated with an arrowhead. (**C**) VSMCs were stained with anti-SMA (red), (**D**) with an anti-Calponin (red) and (**E**) with an anti-NFAC3 (red). Elastin autofluorescence is shown in green. Nuclei are counterstained with DAPI (4',6-diamidino-2-phenylindole, blue). (**F**) TUNEL staining of thoracic aorta cross sections showing apoptotic cells (red) indicated by arrowheads. nuclei stained with DAPI (blue). Scale bar-50 μm.

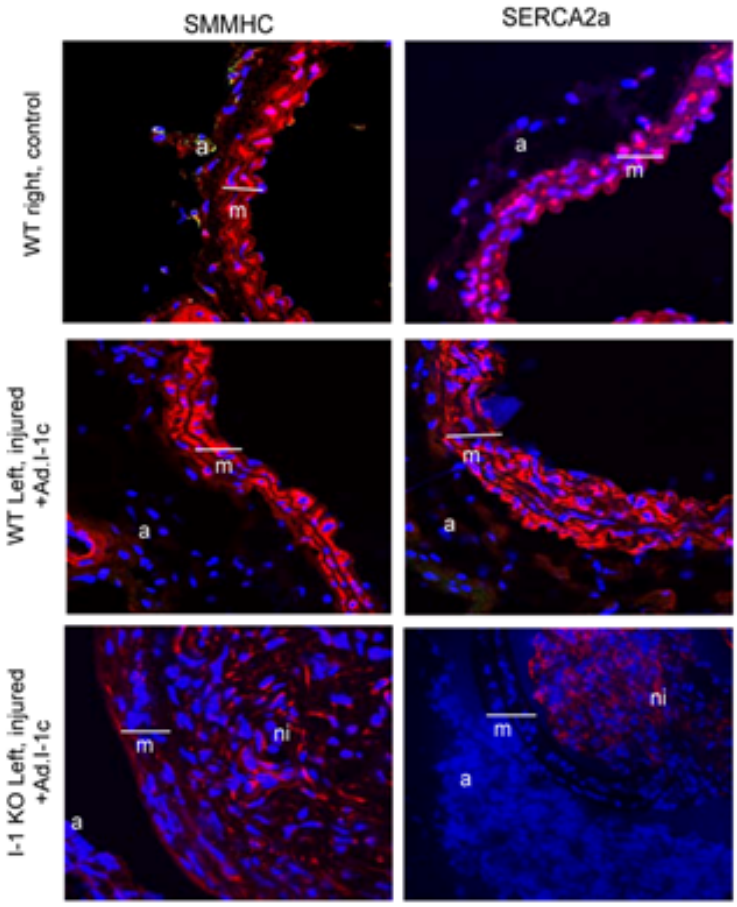

Supplementary Figure 4. **I-1c gene transfer preserves VSMCs contractile phenotype in WT tranduced injured-carotid arteries compared to I-1 KO.** Immunolabeling of control WT right non-injured carotid artery, WT and I-1 KO left injured carotid arteries with anti-SMMHC and anti-SERCA2a (red). Elastin autofluorescence is shown in green and nuclei stained with DAPI (blue). Scale bar-50μm

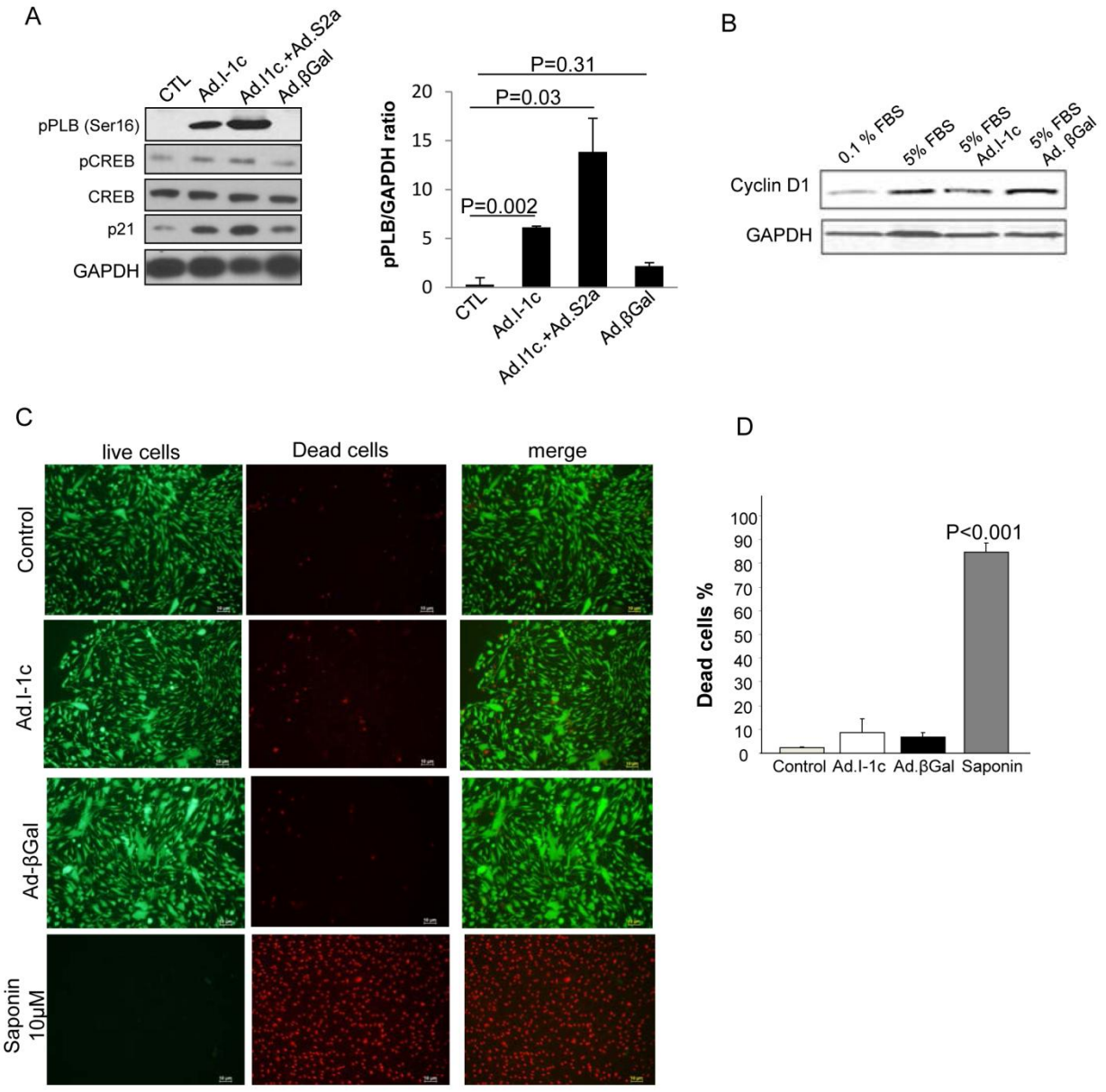

Supplementary Figure 5. Analysis of viability of hCASMC overexpressing I-1c. (**A**) Immunoblot analysis of the effect of I-1c, and Ad.I-1c and Ad.SERCA2a co-expression on pPLB, phosphorylated CREB (pCREB), total CREB and p21 expression levels. Right panel, quantification of the effect of I-1c, and Ad.I-1c and Ad.SERCA2a co-expression on pPLB. (**B**) Western blot analysis of Cyclin D1 in hCASMCs infected with the indicated virus for 4 days. (**C**) Fluorescence microscopy using Calcein AM to determine viable (live) cells in green and ethidium homodimer (EthD1) for non-viable (dead) cells in red. (**D**) Number of dead hCASMCs infected with Ad.I-1c and Ad.βGal, and in saponin (10µM, used as a control) treated cells measured by flow cytometry.

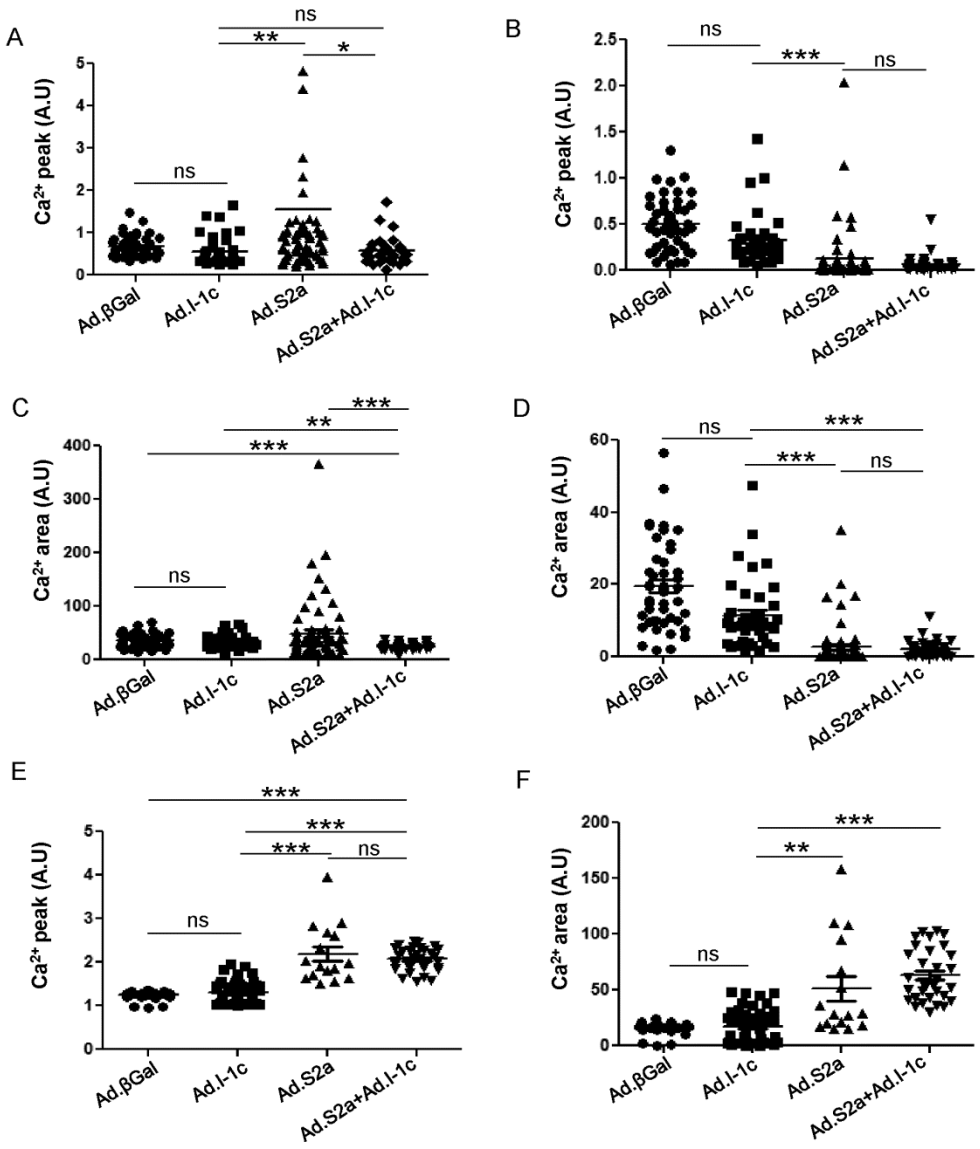

Supplementary Figure 6. Effect of I-1c expression on serum-induced Ca^{2+} transient, SOC and SR store load in synthetic hCASMC. (**A** & **B**) Dot plots comparing the $[Ca^{2+}]$i peak, and (**C**&**D**) $[Ca^{2+}]$i area corresponding to SR Ca^{2+} release and SOC recorded when either serum or extracellular Ca^{2+} (300µM) were added to the cells, respectively. (**E**, **F**) Dot plot comparing the effects of I-1c, SERCA2a or both on SR Ca^{2+} release amplitude and the SR Ca^{2+} store content after thapsigargin (Tg, 1µM) was added to the medium. The $[Ca^{2+}]$i peak corresponding to the maximal SR Ca^{2+} release was recorded when serum was added to the cells cultured in Ca^{2+} free medium. For the Tg experiments, cells were treated, in the absence of extracellular Ca^{2+} (EGTA, 100µM), then Tg was added and Ca^{2+} mobilization was quantified as $\Sigma[Ca^{2+}]$i*time (in sec)/number of measurements (λ $[Ca^{2+}]$Tg*s). The data were recorded along 3 distinct experiments and results were analysed for significance using kruskal-wallis test and all pairs were further analysed using Dunns multiple comparison test. ns-non-significant, *P <0.05, **p<0.001, ***p<0.001.

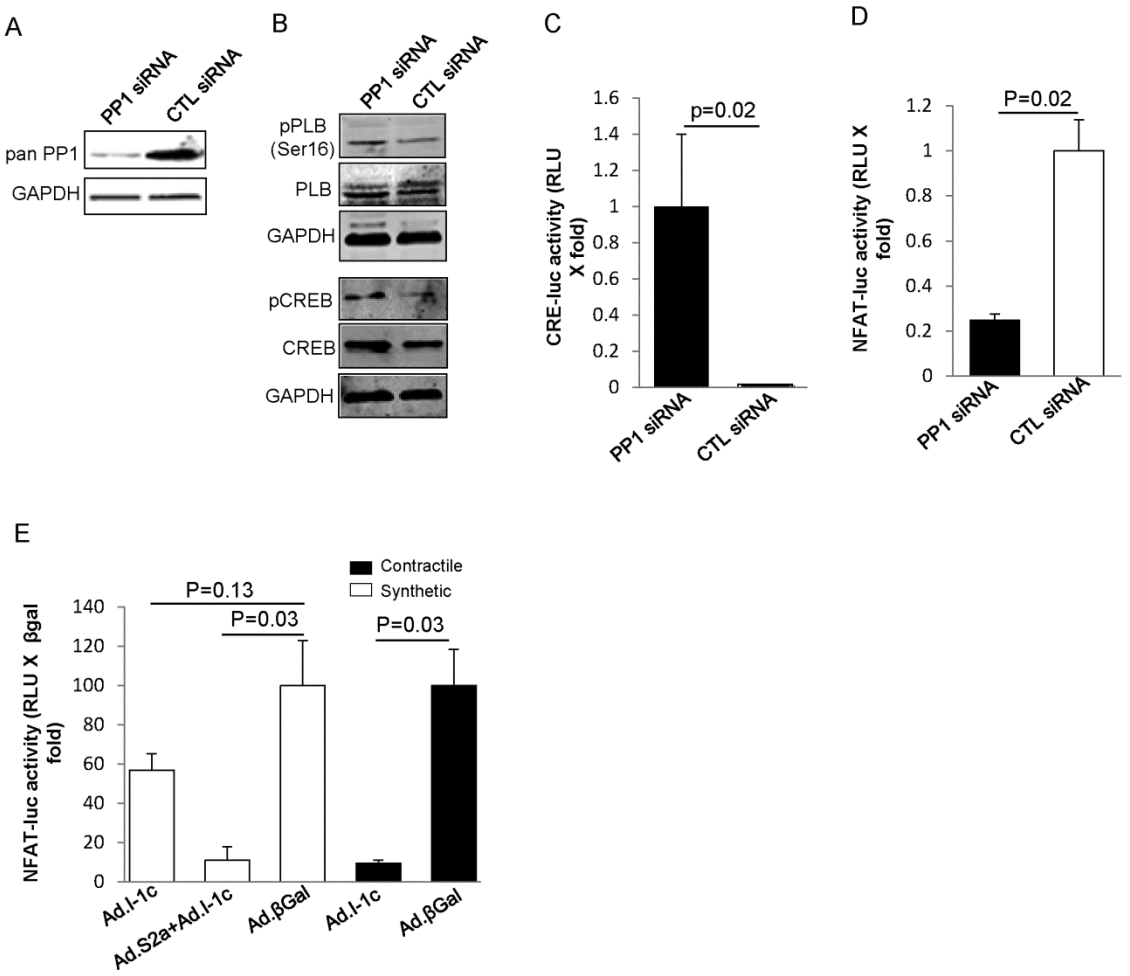

Supplementary Figure 7. Effect of PP1 in PLB and CREB phosphorylation. (**A**) Immunoblot analysis of PP1 protein level in cultured hCASMCs (0.1% FBS) transfected with pan PP1 siRNA and control siRNA for 72 h. (**B**) Effect of siRNA-mediated depletion of PP1 in total and phospho-PLB and CREB in cultured hCAMSCs cells. (**C**) Effects of Pan PP1 siRNA on CRE luciferase activity in cultured hCASMCs (0.1% FBS) transfected with pan PP1 siRNA and control siRNA for 72 h and then infected with an adenovirus expressing CRE-promoter luciferase and (**D**) NFAT-luciferase construct for 48 hours. Data are shown in relative luciferase Units as a percentage of value of control (CTL) siRNA. (**E**) Promoter-reporter assay of NFAT transcriptional activity. Contractile and synthetic cells were infected with indicated adenoviruses during 48h and Ad NFAT-Luc for 48 hours. Data are shown in relative luciferase Units as a percentage of value of Ad.βGal. Values represent mean ± SEM.

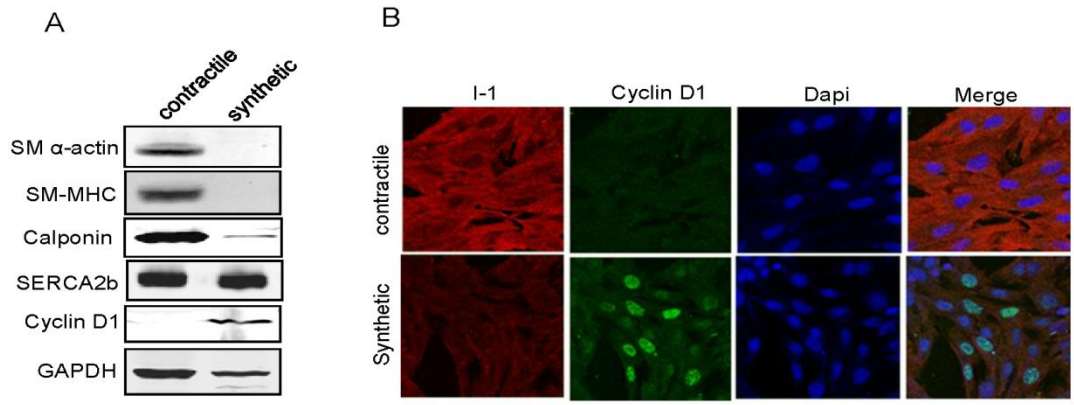

Supplementary Figure 8. I-1 expression in contractile and synthetic rat aortic VSMCs. (**A**) Immunoblot analysis showing relative expression of SM α-actin, SM-MHC, Calponin, SERCA2b and Cyclin D1 in freshly dissociated contractile and synthetic rat VSMCs (passage 4). (**B**) Confocal immunofluorescence of I-1 (red) and Cyclin D1 (green) on freshly dissociated rat contractile aortic and synthetic VSMCs.

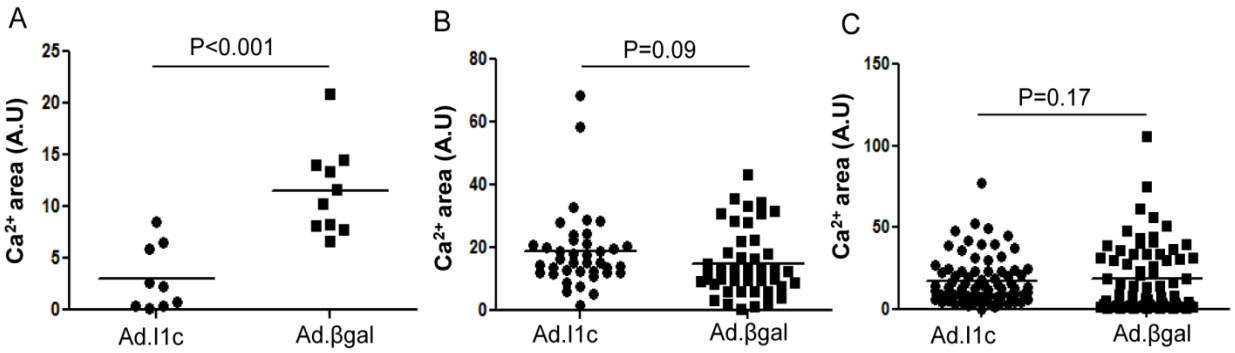

Supplementary Figure 9. Effect of I1c expression on serum-induced Ca^{2+} transient and store content in contractile and synthetic rat aortic VSMC. (**A**) Dot plots comparing the $[Ca^{2+}]$i area corresponding to serum-induced mobilization of SR Ca^{2+} recorded when serum or extracellular Ca^{2+} (300µM) were added to freshly isolated contractile infected with Ad.I-1c or Ad.βGal. (**B**) Effect of I1c on serum-induced mobilization of SR Ca^{2+} in synthetic rat VSMC. (**C**) Dot plots comparing the Ca^{2+} store content after thapsigargin (Tg, 1µM) was added to the medium. Synthetic cells were treated in the absence of extracellular Ca^{2+} (EGTA, 100µM). Then, Tg was added and the following Ca^{2+} mobilization was quantified as $\Sigma[Ca^{2+}]$i*time (in sec)/number of measurements (λ[Ca2+]Tg*s). Mean ± SEM recorded throughout 3 independent experiments.

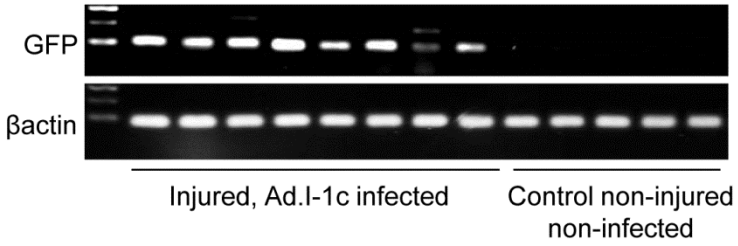

Supplementary Figure 10. Overexpression of I1c prevents vascular remodeling in a rat carotid injury model. PCR analysis demonstrating the presence of GFP DNA in injured carotid segments harvested 14 days after injury compared to control non-injured animals.